1 **Host F-box protein 22 enhances the uptake of *Brucella* by macrophages and**

2 **drives a sustained release of pro-inflammatory cytokines through degradation**

3 **of the anti-inflammatory effector proteins of *Brucella*.**

4

5 **Varadendra Mazumdar[1,2], Kiranmai Joshi[1,2], Binita Roy Nandi[1,2], Swapna Namani[1,2],**

6 **Vivek Kumar Gupta[4, #a], Girish Radhakrishnan[1*]**

7

8 [1]Laboratory of Immunology and Microbial Pathogenesis, National Institute of Animal

9 Biotechnology (NIAB), Hyderabad Telangana 500049, India

10 [2] Regional Centre for Biotechnology (RCB), Faridabad-121001, India

11 Research, Department of Science and Technology, Government of India.

12 [4]ICAR-Indian Veterinary Research Institute (ICAR-IVRI), Izatnagar, India

13 [#a] current address: ICAR-National Research Center on Pig, Guwahati, India

14

15 * Girish Radhakrishnan

16 E-mail: girish@niab.org.in

17

18

19

Author contributions

21   GKR conceived and designed the study. GKR and VM wrote the paper. VM, KJ and BN

22   performed the experiments. SN performed the construction of CRISPR/dCas9 plasmids for

23   downregulation of FBXO22. VKG supervised the experiments with *B. melitensis*. VM and KJ

24   analysed the experimental data. All authors reviewed the results and approved the final version

25   of the manuscript.

Abstract

27   *Brucella* species are intracellular bacterial pathogens, causing the world-wide zoonotic disease,

28   brucellosis. *Brucella* invade professional and non-professional phagocytic cells, followed by

29   resisting intracellular killing and establishing a replication permissive niche. *Brucella* also

30   modulate the innate and adaptive immune responses of the host for their chronic persistence. The

31   complex intracellular cycle of *Brucella* majorly depends on multiple host factors but limited

32   information is available on host and bacterial proteins that play essential role in the invasion,

33   intracellular replication and modulation of host immune responses. By employing an siRNA

34   screening, we identified a role for the host protein, FBXO22 in *Brucella*-macrophage interaction.

35   FBXO22 is the key element in the SCF E3 ubiquitination complex where it determines the

36   substrate specificity for ubiquitination and degradation of various host proteins. Downregulation

37   of FBXO22 by siRNA or CRISPR-Cas9 system, resulted diminished uptake of *Brucella* into

38   macrophages, which was dependent on NF-κB-mediated regulation of phagocytic receptors.

39   FBXO22 expression was upregulated in *Brucella*-infected macrophages that resulted induction

40   of phagocytic receptors and enhanced production of pro-inflammatory cytokines through NF-κB.

41   Furthermore, we found that FBXO22 recruits the effector proteins of *Brucella*, including the

42   anti-inflammatory proteins, TcpB and OMP25 for degradation through the SCF complex. We did

43   not observe any role for another F-box containing protein of SCF complex, β-TrCP in *Brucella*-

44   macrophage interaction. Our findings unravel novel functions of FBXO22 in host-pathogen

45   interaction and its contribution to pathogenesis of infectious diseases.

Author Summary

47   Brucellosis is a major zoonotic disease world-wide that poses a serious veterinary and public

48   health problem in various countries, impacting their economic development. Brucellosis is

49   caused by the species of intracellular bacterial pathogen, *Brucella* that replicates in professional

50   and non-professional phagocytic cells. *Brucella* is considered as a stealthy pathogen as it

51   invades/suppresses host defense responses using various virulence strategies. *Brucella* hijacks

52   many cellular processes for gaining entry into the target cells, followed by establishing a

53   replication permissive niche. However, host proteins that are involved in *Brucella*-macrophage

54   interaction remains obscure. Here, we identified the host protein, FBXO22 that recruits target

55   proteins to SCF E3 ubiquitination complex for their ubiquitination and degradation. We found

56   that down-regulation and upregulation of FBXO22 decreased and enhanced the uptake of

57   *Brucella* by macrophages, respectively. Our subsequent studies revealed that *Brucella* induces

58   the expression of FBXO22 that resulted activation of NF-κB and the concomitant upregulation of

59   phagocytic receptors that might have contributed to the enhanced uptake of *Brucella*. The

60   *Brucella*-induced expression of FBXO22 resulted enhanced production of pro-inflammatory

61   cytokines. We have also found that FBXO22 targets *Brucella* effectors, including the anti-

62   inflammatory effector proteins for degradation through the SCF complex. Our experimental data

63   reveals that FBXO22 plays an important role in the uptake of microbial pathogens by

3

64   macrophages and pathogenesis of infectious diseases that is resulting from overt inflammatory

65   responses.

Introduction

67   *Brucella* species are Gram negative facultative intracellular bacterial pathogens that cause the

68   world-wide zoonotic disease, brucellosis (1). Brucellosis specifically impacts low-income

69   countries and it is considered as one of the leading neglected zoonotic diseases in the world. The

70   domestic and wild animals are the primary hosts for *Brucella* and the human infections generally

71   occurs through inhalation of aerosolized bacteria and ingestion of *Brucella* contaminated dairy

72   products. Brucellosis remains a major threat to public health and livestock productivity in

73   various countries leading to enormous economic loss. *Brucella* species are reported to cause

74   500,000 new infections every year and some of the species are considered as potential agents for

75   bioterrorism (1, 2). The symptoms of human brucellosis includes undulating fever, chills,

76   headache and joint pain. Brucellosis has also been reported to cause arthritis, spondylitis,

77   epididymo-orchitis, acute renal failure, endocarditis, splenic abscess, abortion, and

78   neurobrucellosis (3). There are no human vaccines for brucellosis and the antibiotic treatment for

79   brucellosis is complex due to prolonged treatment regimen with multiple antibiotics and frequent

80   occurrence of relapses (4). There are four species of *Brucell*a *viz. B. melitensis*, *B. abortus*, *B.*

81   *suis* and *B. canis* that are reported to infect human (5).

82   *Brucella* successfully invades and multiplies in professional and non-professional macrophages

83   and trophoblasts (6). After invading the target cells, *Brucella* escapes intracellular killing by

84   preventing the fusion of *Brucella*-containing phagosomes with lysosomes (7). Subsequently, the

85   *Brucella*-containing phagosomes fuse with the endoplasmic reticulum and acquires ER-derived

4

86   membrane and these vacuoles act as the replication permissive niche for *Brucella* (8).

87   Compared to other microbial pathogens, minimal information is available on virulence strategies

88   of *Brucella* as they do not express classical virulence factors such as plasmids and toxins (9).

89   The host factors that support the invasion and intracellular multiplication of *Brucella* are also

90   remain poorly understood. To date very few host proteins *viz*. IRE1α, Rho1, Rac2, Cdc42 and

91   Sar1 have been implicated in the infection process of *Brucella* (10). Therefore, it is essential to

92   identify the host factors that are targeted by *Brucella* to manipulate various cellular processes to

93   facilitate its invasion, intracellular replication and chronic persistence in the host. These host

94   factors could serve as potential targets to develop improved drugs for brucellosis.

95   The F-box protein 22 (FBXO22) is a part of multi-protein ubiquitin ligase complex termed as

96   SCF. This complex constitutes S phase kinase-associated protein 1 (SKP1), Cullin 1 (CUL1), F-

97   box protein (FBXO) and the Ring box protein 1 (RBX1). The CUL1 acts as a scaffolding protein

98   where its amino terminus binds with SKP1 and the carboxyl terminus binds to the RBX1, which

99   is associated with the E2 enzyme (11). This complex mediates the transfer of ubiquitin moiety

100   from E2 enzyme to the substrate protein. The F-box-protein component of SCF has been

101   reported to determine the substrate specificity of the SCF complex (12). One of the F-box

102   proteins, β-TrCP is known to mediate ubiquitination and degradation of IκBα through SCF

103   complex, which activates the key transcription factor, NF-κB that is involved in many cellular

104   responses. FBXO22 has been reported in promotion and metastasis of various cancers including

105   hepatocellular carcinoma, osteosarcoma and lung cancer (13-18). On the other hand, it has been

106   reported to suppress human renal cell carcinoma and metastasis of breast cancer (19, 20).

107   FBXO22 was also implicated in estrogen receptor modulation and the regulation of senescence

108   by methylating p53 (21-23). The effector protein of *S. typhimurium,* GogB has been reported to

109   target FBXO22 to suppress secretion of pro-inflammatory cytokines. The GogB interacts with

110   and inhibits the functions of SKP1 and FBXO22 proteins to prevent the degradation of IκBα,

111   resulting in the inhibition of NF-κB activation and secretion of pro-inflammatory cytokines that

112   minimize the tissue damage during *S. typhimurium* infection (24).

113   Here we report that FBXO22 plays an important role in the invasion of *Brucella* into

114   macrophages. Down regulation and overexpression of FBXO22 in macrophages resulted

115   diminished and enhanced invasion of *Brucella* into macrophages, respectively. Further, we

116   observed that *Brucella* upregulates FBXO22 in the infected macrophages that leads to the

117   enhanced secretion of TNF-α through NF-κB activation. Our experimental data suggests that

118   FBXO22 plays an essential role in the pathogenesis of brucellosis.

119   **Results**

120   **FBXO22 contributes to the macrophage infection of *Brucella*.**

121   We identified the role of FBXO22 in the *Brucella* infection of macrophages while performing an

122   siRNA screening using *B. neotomae*, which has been considered as the model pathogen to study

123   brucellosis (25). *B. neotomae* is a BSL-2 pathogen that exhibits the infection dynamics of the

124   BSL-3 counterpart, *B. melitensis* (26). We could recover a diminished number of *B. neotomae*

125   from the J774 macrophages treated with siFBXO22 compared to the cells treated with non-target

126   (NT) siRNA (Fig. 1A and Fig.S1 A&B). To examine the effect of FBXO22 further, we analyzed

127   the CFU at various times post-infection that also resulted recovery of decreased number of *B.*

128   *neotomae* from the siFBXO22 treated cells (Fig. 1B). Next, siFBXO22 or non-target siRNA

129   treated J774 macrophages were infected with *B. neotomae* expressing GFP, followed by

130   analyzing the cells by confocal microscopy, 24 hours post-infection. The macrophages treated

6

131   with siFBXO harbored less number of *B. neotomae*-GFP compared to the cells treated with the

132   control non-target siRNA (Fig 1C). To confirm the experimental data further, we overexpressed

133   FBXO22 in J774 macrophages, followed by infection with *B. neotomae* and enumeration of CFU

134   at various times post-infection. In agreement with the previous observation, we could recover

135   more bacteria from the J774 cells overexpressing FBXO22 compared to the cells transfected

136   with empty vector alone (Fig. 1D and Fig.S1 C). These experimental data clearly suggest that

137   FBXO22 plays an important role in *Brucella* infection of macrophages.

138   **FBXO22 supports the invasion of *Brucella* into macrophages**

139   We observed diminished and elevated levels of *B. neotomae* in FBXO22-silenced and-

140   overexpressed macrophages, respectively, at all the time points that we examined. Therefore, we

141   sought to examine whether FBXO22 plays any role in the invasion of *Brucella* into

142   macrophages. To analyze this, *Brucella* invasion assay (27)(28) was performed using the *B.*

143   *neotomae*. The siFBXO22 or non-target siRNA treated J774 macrophages were infected with *B.*

144   *neotomae* for 30 minutes, followed by gentamycin treatment for 30 minutes and enumeration of

145   CFU (Fig. 2A). We observed a decreased invasion of *B. neotomae* into macrophages treated with

146   siFBXO22 compared to cells treated with non-target siRNA. To confirm the experimental data

147   further, siFBXO22 or non-target siRNA treated J774 cells were infected with *B. neotomae*-GFP,

148   followed by gentamycin treatment and analyzing the invasion of *B. neotomae-GFP* by confocal

149   microscopy (Fig. 2B). In agreement with the CFU data, a decreased number of *B. neotomae*-GFP

150   was observed in the cells treated with siFBXO22. The infection of siFBXO22 or non-target

151   siRNA treated J774 cells for 60 or 90 minutes, followed by 30 minutes of gentamycin treatment

152   also showed diminished invasion of *B. neotomae* in siFBXO22 treated cells (Fig. 2A). In order to

153   confirm the role of FBXO22 further, we overexpressed FBXO22 in J774 macrophages followed

7

154   by *Brucella* invasion assay. The J774 cells overexpressing FBXO22 showed more number of *B.*

155   *neotomae* compared to the cells transfected with the empty vector (Fig 2C). β-TrCP is another F-

156   box containing protein, which is associated with the SCF ubiquitin ligase complex.

157   Overexpression of β-TrCP did not affect the invasion of *B. neotomae* into macrophages (Fig.

158   2D).

159   To validate the experimental data obtained from the siRNA-mediated silencing, we

160   transcriptionally suppressed the expression of FBXO22 in J774 or iBMDMs using a

161   CRISPR/dCas9 system. Four guide RNAs (gRNAs) from the Transcriptional Start Site (TSS) of

162   FBXO22 was designed and synthesized, followed by cloning them into the CRISPR/dCas9

163   expression plasmid, which harbored the dead Cas9 that lacks DNA nickase activity (29) . The

164   guide RNA directs the dCas9 to the TSS of FBXO22 that prevents its transcription. First, we

165   evaluated the efficiency of all the four gRNAs and selected gRNA-3 that showed maximum

166   suppression of FBXO22 (Fig. 2E & F) (Fig.S1 D). Next, we transfected J774 or iBMDMs with

167   the CRISPR-dCas9-FBXOgRNA-3 expression plasmid followed by infection studies using *B.*

168   *neotomae*. In agreement with the previous findings, transcriptional suppression of FBXO22 in

169   macrophages using CRISPR/dCas9 system also resulted a diminished invasion of *B. neotomae*

170   (Fig. 2G). To examine the requirement of FBXO22 for the invasion of another pathogenic

171   species of *Brucella,* we performed the infection studies with *B. melitensis.* J774 macrophages

172   were transfected with CRISPR-dCas9-FBXOgRNA-3, followed by infection with *B. melitensis*

173   and CFU enumeration. Similar to *B. neotomae*, *B. melitensis* also exhibited a defective invasion

174   in the FBXO22 knock-down macrophages (Fig 2H). The experimental data confirm that

175   FBXO22 plays an essential role in the invasion of *Brucella* into macrophages.

176   The effector protein of *Salmonella*, GogB is reported to interact and inhibit the functions of

177   FBXO22 to suppress the inflammation (24). Therefore, we examined if the inhibition of

178   FBXO22 by GogB could impact the FBXO22-mediated entry of *Brucella*. We observed a

179   diminished invasion of *B. neotomae* into macrophages that are overexpressing FBXO22 and

180   GogB compared to the cells over-expressing FBXO22 alone (Fig 2 I), which further confirmed

181   the role of FBXO22 in the invasion of *Brucella* into macrophages.

182   ***Brucella* infection induces upregulation of FBXO22 and activation of NF-κB in**

183   **macrophages.**

184   Given that FBXO22 contributes to the invasion of *Brucella* into macrophages, we wished to

185   examine whether *Brucella* infection induces the expression of FBXO22 in macrophages. To

186   examine this, J774 macrophages were infected with *B. neotomae,* followed by harvesting the

187   cells at various time points after the infection and analyzing the expression of FBXO22 by qRT-

188   PCR and immunoblotting (Fig 3A & B). We observed elevated levels of FBXO22 in *B.*

189   *neotomae* infected macrophages with increasing time points. The induction of FBXO22

190   expression was observed as early as 30 minutes post-infection in the *B. neotomae* infected

191   macrophages (Fig. 3C). Similarly, the infection with *B. melitensis* also induced upregulation of

192   FBXO22 at early and late time points (Fig. 3D). Next, we wished to examine whether *Brucella*

193   infection induces the expression of β-TrCP also. The expression level of β-TrCP was analyzed

194   by qRT-PCR at different time points after *B. neotomae* infection in J774 cells. No significant

195   difference in the expression of β-TrCP was observed in *B. neotomae* infected J774 cells

196   compared to the uninfected cells at all-time points (Fig.S2). To examine, whether the FBXO22

197   expression is upregulated by other stimulants, we treated J774/iBMDM with *E. coli* LPS,

198   followed by quantifying the levels of FBXO22 at various time points after induction. We found

9

199   that LPS could also induce the expression of FBXO22, which may be required for the activation

200   of NF-κB and production of pro-inflammatory cytokines (Fig. 3E &F).

201   FBXO22 has been reported to target multiple proteins for degradation by means of ubiquitination

202   by the SCF complex (13, 16, 20, 30). One of the targets of FBXO22 is reported to be β where the

203   degradation of IκBα relieves the NF-κB inhibition that leads to its nuclear localization and

204   transactivation of various genes (24). In agreement with this, we observed an enhanced

205   degradation of IκBα upon overexpression of FBXO22 (Fig.S3). Since we found the induction of

206   FBXO22 in *Brucella*-infected macrophages, we wished to examine whether the *Brucella*-

207   induced upregulation of FBXO22 leads to the activation of NF-κB using a luciferase-based NF-

208   κB reporter assay. RAW264.7 macrophages were transfected with luciferase reporter plasmids,

209   followed by infection with *B. neotomae* and harvesting the cells at various time points.

210   Subsequently, the cells were lysed and the luciferase activity was measured. We observed an

211   enhanced luciferase activity in *Brucella*-infected macrophages that indicated the activation of

212   NF-κB (Fig. 4A). To confirm the experimental data further, we analyzed the level of IκBα in the

213   *B. neotomae* infected macrophages. We found an enhanced degradation of IκBα in the *B.*

214   *neotomae*-infected macrophages compared to the uninfected cells (Fig 4B). Taken together the

215   experimental data imply that *B. neotomae* upregulates FBXO22 that in turn induces the

216   activation of NF-κB.

217   NF-κB has been reported to play an essential role in the uptake of bacteria by macrophages (31).

218   Therefore, we sought to examine whether the inhibition of NF-κB affects the invasion of

219   *Brucella* into macrophages. We treated macrophages with the NF-κB inhibitor, BAY 11-7082,

220   followed by infection with *B. neotomae* or *B. melitensis* to analyze its invasion. We observed a

221   significantly diminished invasion of *B. neotomae* or *B. melitensis* into the macrophages that are

10

222   treated with BAY 11-7082 (Fig. 4C & D). To confirm the data further, we treated macrophages

223   overexpressing FBXO22 with BAY 11-7082 or DMSO, followed by infection with *B. neotomae*.

224   We found a decreased invasion of *B. neotomae* into the FBXO22 overexpressed macrophages

225   treated with BAY 11-7082 compared to DMSO treated cells (Fig 4E). Taken together, our

226   experimental data suggest that the intracellular invasion of *Brucella* upregulates FBXO22, which

227   activates NF-κB that in turn, enhances the uptake of *Brucella*.

228   **FBXO22-mediated NF-κB activation upregulates scavenging receptors on macrophages.**

229   The scavenger receptors (SRs) and C-type lectin receptors have been reported to play an

230   essential role in the phagocytosis of various microorganisms (32-35). Since the upregulation of

231   FBXO22 and the resulting activation of NF-κB enhanced the invasion of *Brucella* into

232   macrophages, we sought to examine whether FBXO22-mediated NF-κB activation promotes the

233   expression levels of SRs on macrophages. It has been previously reported that the cellular prion

234   protein (PrPc) is essential for internalization of *Brucella* (36). The NF-κB has been reported to

235   regulate the expression of various phagocytic receptors such as macrophage scavenger receptor-1

236   (MSR1), DC-SIGN, Dectin-1 and CD36 that are involved in bacterial phagocytosis (37). We

237   examined the expression levels of phagocytic receptors by qRT-PCR in the macrophages that are

238   downregulating or overexpressing FBXO22. We found diminished expression of Dectin-1, DC-

239   SIGN, CD36, PrPc and MSR-1 in the FBXO22 knock-down macrophages. The overexpression

240   of FBXO22 resulted upregulation of all the receptors except for Dectin-1. The macrophages

241   treated with BAY 11-7082 exhibited diminished expression of scavenger receptors, indicating

242   the role of NF-κB in regulating these receptors (Fig. 5A &B, C).

243   Next, we examined whether *Brucella* infection could upregulate these receptors in the

244   macrophages. iBMDMs were infected with *B. neotomae*, followed by harvesting the cells at 2, 4

245   and 8 hours post-infection and analyzing the expression of phagocytic receptors by qRT-PCR.

246   We observed an upregulation of DC-SIGN, CD36, PrPc and MSR-1 expression in the

247   macrophages at 4 hours post-infection (Fig. 5D). Next, we examined whether the upregulation of

248   phagocytic receptors enhances the uptake of *Brucella* into macrophages. iBMDM were infected

249   with *B. neotomae* for 2 or 4 hours, followed by re-infection with *B. neotomae*/*B. neotomae*

250   expressing td-tomato for 30 minutes and enumeration of CFU and confocal microscopy. We

251   observed an enhanced invasion of *B. neotomae*- in the macrophages that were re-infected 4-hours

252   post-infection compared to 2-hour time point (Fig. 5E). The infection of macrophages with *B.*

253   *neotomae/ B. neotomae*-GFP for 2 or 4 hours, followed by re-infection with *B. neotomae*-td

254   tomato for 30 minutes also indicated an enhanced invasion of *B. neotomae* td-tomato at 4-hours

255   post-infection (Fig. 5F & Fig.S4). Taken together, the experimental data suggest that the

256   induction of FBXO22 upregulates phagocytic receptors through NF-κB and these receptors

257   mediate an enhanced uptake of *Brucella* into the macrophages.

258   **Brucella-induced upregulation of FBXO22 results in enhanced secretion of TNF-α by**

259   **macrophages.**

260   We observed that FBXO22 is upregulated by *Brucella*, which activated NF-κB through the

261   degradation of IκBα. Activation of NF-κB leads to the secretion of various pro-inflammatory

262   cytokines including the TNF-α and IL-6. TNF-α is reported to play an important role in the

263   pathogenesis of brucellosis, including the induction of abortion. Therefore, we sought to examine

264   whether *Brucella*-induced NF-κB activation leads to the enhanced secretion of pro-inflammatory

265   cytokines by infected macrophages. J774 macrophages were infected with *B. neotomae* or *B.*

266   *melitensis,* followed by harvesting cells and culture supernatants at various times post-infection.

267   Subsequently, the amounts of secreted TNF-α and IL-6 were quantified by qRT-PCR and

268   ELISA. We observed an enhanced expression and secretion of TNF-α and IL-6 in the *B.*

269   *neotomae or B. melitensis*-infected macrophages with increasing time points (Fig. 6A-F). Next,

270   we wished to examine whether the induction of TNF-α is mediated through FBXO22. To

271   examine this, FBXO22 was overexpressed in J774 cells, followed by infection with *B. neotomae*

272   and quantification of secreted TNF-α and IL-6 in culture supernatants at various time points. We

273   observed an enhanced TNF-α and IL-6 secretion by the FBXO22 overexpressing macrophages

274   compared to the empty vector transfected cells (Fig. 6G & H). The treatment of FBXO22

275   overexpressing macrophages with BAY 11-7082 decreased the production of TNF-α and IL-6

276   compared to the DMSO treated cells, suggesting that NF-κB mediates the induction of pro-

277   inflammatory cytokines in FBXO22 overexpressing macrophages (Fig. 6 I & J). Further, we

278   analyzed the *Brucella*-induced secretion of TNF-α and IL-6 in FBXO22 knock-down

279   macrophages. J774 cells were transfected with CRISPR-dCas9-FBXOgRNA-3 expression

280   plasmid (FBXO22CR) or empty vector, followed by infection with various multiplicity of

281   infection (MOI) of *B. neotomae* and quantification of TNF-α and IL-6 at 12 hours post-infection.

282   The FBXO22 knock-down macrophages secreted significantly reduced level of TNF-α and IL-6

283   at all the MOI compared to the empty vector transfected macrophages (Fig.S5 A&B). In order to

284   confirm further that the induction of pro-inflammatory cytokines are mediated by NF-κB, we

285   treated iBMDMs with BAY 11-7082, followed by infection with different MOI of *B. neotomae*

286   and quantification of TNF-α and IL-6 levels by qRT-PCR. BMDMs treated with BAY 11-7082

287   secreted diminished level of TNF-α and IL-6 at all the MOI compared to the untreated cells (Fig.

288   6K& L). The experimental data suggest that *B. neotomae* upregulates FBXO22, which in turn

289   induces the activation of NF-κB and the secretion of TNF-α and IL-6. The enhanced secretion of

290   TNF-α by *Brucella*-infected cells may contribute to the induction of abortion in brucellosis.

13

FBXO22 induces degradation of effector proteins of *Brucella*.

Brucella is reported to encode two anti-inflammatory proteins, such as TIR domain containing protein (TcpB) and outer membrane protein 25 (OMP25). TcpB is reported to efficiently suppress NF-κB activation and pro-inflammatory cytokine secretion mediated by Toll-like Receptor 2 and 4. OMP25 also attenuates secretion of pro-inflammatory cytokines in the *Brucella*-infected macrophages (38). An enhanced level of pro-inflammatory cytokines has been reported in mice infected with TcpB or OMP25 knock-out *Brucella* (39). However, in the *Brucella*-infected macrophages, the upregulation of FBXO22 resulted in enhanced activation of NF-κB and elevated expression of TNF-α. Therefore, we wished to examine how the FBXO22-mediated induction of TNF-α occurs in the presence of anti-inflammatory effector proteins of *Brucella*. Since FBXO22 serves as the component of SCF E3 ubiquitin ligase complex where it recruits the target proteins for ubiquitination and degradation, we sought to examine whether FBXO22 targets TcpB and OMP25 also for degradation. First, we analyzed whether FBXO22 interacts with TcpB by co-immunoprecipitation assay. The lysate of HEK293T cells overexpressing FLAG-FBXO22 was incubated with purified MBP-TcpB fusion protein or MBP alone, followed by immunoprecipitation of FBXO22 using anti-FLAG antibody. The MBP-TcpB was co-immunoprecipitated with FLAG-FBXO22, suggesting a potential interaction between FBXO22 and TcpB (Fig.7A). MBP alone was not detected in the immunoprecipitated samples, which indicated specific interaction between FBXO22 and TcpB. Next, we examined whether FBXO22 targets TcpB for degradation. HEK293T cells were co-transfected with equal concentration of TcpB and increasing concentrations of FBXO22. Interestingly, we observed an enhanced degradation of TcpB with increasing concentrations of FBXO22 (Fig. 7B).

14

313   To further confirm the role of FBXO22 in the degradation of TcpB, we silenced FBXO22 in

314   HEK293T cells, followed by analyzing the degradation of transiently expressed TcpB. The

315   transfection of HEK293T cells with siFBXO22 resulted a significant silencing of FBXO22,

316   which was confirmed by qRT-PCR and immunoblotting (Fig. 7C & D). We found a diminished

317   degradation of TcpB in the FBXO22 silenced cells compared to the cells transfected with the

318   non-target siRNA control (Fig.7D). Next, we examined whether *Salmonella*-mediated inhibition

319   of FBXO22 through GogB prevents the degradation of TcpB. To analyze this, HEK293T cells

320   were co-transfected with FBXO22 and TcpB, followed by infecting the cells with *Salmonella*

321   *typhimurium* and analyzing the degradation of TcpB. We observed a diminished degradation of

322   TcpB by FBXO22 in the *S. typhimurium*-infected cells compared to the uninfected control (Fig.

323   7E).

324   In order to confirm that FBXO22 degrades TcpB through the SCF complex, we analyzed the

325   degradation of TcpB in SKP1 silenced HEK293T cells. The SKP1 serves as an adaptor protein

326   for SCF complex, which is essential for the recognition and binding of F-box proteins (12, 40).

327   HEK293T cells were transfected with siSKP1 and the silencing of SKP1 was confirmed by qRT-

328   PCR (Fig. 7F). Next, SKP1 silenced cells were co-transfected with TcpB and FBXO22

329   expression plasmids, followed by analyzing the degradation of TcpB. We observed a diminished

330   degradation of TcpB in the SKP1 silenced cells compared to the non-target siRNA control (Fig.

331   7G). Next, we examined whether the other F-box-containing protein, β-TrCP also recruits TcpB

332   for degradation through SCF complex. Co-transfection of HEK293T cells with TcpB and

333   increasing concentrations of β-TrCP did not result the degradation of TcpB (Fig. 7H). The

334   recruitment of proteins to SCF complex by FBXO22 leads to their ubiquitination and

335   degradation. Therefore, we examined the ubiquitination of TcpB in the presence of FBXO22.

15

336   HEK293T cells were co-transfected with MYC-FBXO22, FLAG-TcpB and HA-ubiquitin,

337   followed by immunoprecipitation of FLAG-TcpB and immunoblotting. Ubiquitin-conjugated

338   FLAG-TcpB was detected by probing the membrane with anti-HA antibody. We observed an

339   enhanced ubiquitination of TcpB in the presence of FBXO22 (Fig. 7I). These experimental data

340   clearly indicate that FBXO22 recruits TcpB to the SCF complex for its ubiquitination and

341   degradation.

342   Next, we analyzed the degradation of OMP25 by FBXO22 by co-transfection experiment. As we

343   observed in the case of TcpB, we found the degradation of OMP25 also by FBXO22 in a dose

344   dependent manner (Fig. 7J). In order to examine whether FBXO22 targets only the anti-

345   inflammatory effector proteins of *Brucella*, we performed co-transfection experiment with

346   another effector proteins, Bsp1. Interestingly, FBXO22 induced degradation of Bsp1 also in a

347   dose dependent manner (Fig. 7K). In agreement with the previous findings, β-TrCP did not

348   induce degradation of Bsp1 (Fig. S6). The experimental data suggest that FBXO22 promotes

349   degradation of *Brucella* effector proteins in the macrophages.

Discussion

351   *Brucella* is considered as a stealthy bacterial pathogen and it efficiently manipulates various host

352   cellular process for its invasion and intracellular replication. However, the host proteins that are

353   targeted by *Brucella* to infect the macrophages remain obscure. In this study, we demonstrate

354   that the FBXO22, which is a F-box containing substrate binding protein of SCF E3 ubiquitin

355   ligase, contributes to the invasion of *Brucella* into the macrophages. FBXO22, serves as the

356   substrate recognition subunit of SCF complex and it has been implicated in regulating many

357   cellular processes by ubiquitination and subsequent degradation of target proteins (17). FBXO22

358   has been reported to be involved in driving the tumor progression and metastasis in many cancer

359   cells (30). Deletion of FBXO22 caused instability of SCF complex leading to suppression of

360   tumor progression (17). Our experimental data revealed an additional role for FBXO22, where it

361   enhanced the uptake of *Brucella* by macrophages and induced the upregulation of pro-

362   inflammatory cytokines through NF-κB activation.

363   The receptors on macrophages such as Dectin-1, DC-SIGN; and the scavenger receptors, MSR-1

364   and CD36 are reported to play essential role in the uptake and TLR-independent signaling of

365   various bacterial pathogens (41-43). These receptors are involved in host defense by

366   phagocytosis of various microbial pathogens for intracellular killing (41). However, some

367   pathogenic microorganisms use these receptors as Trojan horses for host dissemination. An

368   enhanced uptake of both Gram positive and Gram negative bacteria have been observed in HeLa

369   cells overexpressing CD36 (42). Various bacterial, protozoan and viral pathogens have been

370   reported to hijack DC-SIGN on dendritic cells and macrophages for host dissemination and

371   pathogenicity (43-48). Studies have demonstrated that NF-κB is required for phagocytosis of

372   bacteria where induction of NF-κB by PAMPS derived from the phagosomal degradation of

373   internalized bacteria could induce the expression of phagocytic receptors (31). Treatment of

374   macrophages with resveratrol, one of the known inhibitors of NF-κB, hampered the phagocytosis

375   of bacteria by lowering the expression levels of phagocytic receptors (37). In agreement with

376   these finding, our studies also showed downregulation of phagocytic receptors in presence of the

377   NF-κB inhibitor, BAY 11-7082. The FBXO22 knock-down macrophages also expressed lower

378   levels of phagocytic receptors, which imply that FBXO22-mediated NF-κB activation is required

379   for enhanced expression of phagocytic receptors. It has also been reported that PrPC plays a

380   crucial role in the uptake of *B. abortus* by macrophages (36). We observed that NF-κB is

381 activated by *Brucella* and the inhibition of NF-κB using the chemical inhibitor, BAY 11-7082

382 affected the invasion of *Brucella* into macrophages. *Brucella* infection of macrophages induced

383 the expression of various phagocytic receptors through FBXO22-mediated activation of NF-κB.

384 We observed a maximum induction of these receptors at 4 hours post-infection. Various

385 macrophage infection studies have reported a sharp decline of *Brucella* CFU at 4-hours post

386 infection owing to the killing of 90% of the invaded bacteria (49). This may release various

387 PAMPs, which can activate intracellular PRRs and the concomitant induction of NF-κB, which

388 may upregulate the expression of phagocytic receptors. The enhanced uptake of *Brucella* during

389 re-infection at 4-hours post-infection clearly indicates that *Brucella* employ these phagocytic

390 receptors to invade the macrophages. Further, the overexpression of FBXO22 resulted

391 upregulation of various phagocytic receptors that positively correlated with bacterial invasion

392 and replication. Taken together, the experimental data suggest that *Brucella* targets these

393 receptors for invasion, followed by resisting intracellular killing and establishing a replication

394 permissive niche.

395 Activation of NF-κB in macrophages is reported to be an antimicrobial immune response, which

396 leads to transient inflammation during early stages of infection (50). NF-κB serves as the central

397 mediator of various pro-inflammatory cytokines including TNF-α. We observed induction of

398 NF-κB and the resulting upregulation of TNF-α in the *Brucella*-infected macrophages. The

399 elevated levels of TNF-α in the *Brucella*-infected macrophages correlated with upregulation of

400 FBXO22. Overexpression of FBXO22 enhanced the *Brucella* induced secretion of TNF-α, which

401 was sensitive to BAY 11-7082 treatment, indicating the requirement of NF-κB activation for

402 TNF-α production. The role of *Brucella*-mediated upregulation of FBXO22 in the production of

403 TNF-α was further demonstrated in FBXO22 knock-down cells where the infection with

18

404   increasing MOI of *Brucella* did not result an enhanced TNF-α production compared to the

405   control. The elevated levels of pro-inflammatory cytokines is a hall mark of *Brucella* infection,

406   which contributes to the *Brucella*-induced abortion (51, 52). The average levels of cytokines

407   such as TNF-α, IFN-γ and IL-12 are reported to be higher in *B. abortus* infected BALB/c mice

408   compared to the mice infected with *Yersinia enterocolitica* (53). In contrary, the attenuation of

409   pro-inflammatory responses by blocking the function of FBXO22 has been reported in

410   *Salmonella* (24). *Salmonella* secretes the effector protein, GogB, which shares the similarity with

411   the F-box motif of human FBXO22 that is required for its binding with SKP1. GogB is reported

412   to outcompete FBXO22 that prevents degradation of IκBα, resulting inhibition of NF-κB and

413   subsequent suppression of pro-inflammatory cytokines (24). Infection of mice with GogB

414   deficient *Salmonella* resulted elevated pro-inflammatory responses and enhanced colonization in

415   the gut. We found that GogB mediated inhibition of FBXO22 affected the uptake of *Brucella* by

416   macrophages. However, the GogB is reported to have no role in replication of *Salmonella* in

417   macrophages and in epithelial cells. Taken together, it can be speculated that FBXO22-mediated

418   enhanced production of pro-inflammatory cytokines contributes to the host damage due to

419   overacted inflammatory responses.

420   SCF E3 ubiquitin ligase complex is responsible for strict turnover of proteins by their

421   polyubiquitin-mediated degradation. The substrate specificity of SCF complex largely depends

422   on the distinct F-box proteins (54). Since the FBXO22 is a part of SCF E3 Ubiquitin ligase

423   complex, we analyzed the recruitment of *Brucella* effector proteins to SCF by FBXO22 for

424   degradation. *Brucella* encode two reported anti-inflammatory proteins, *viz.* TcpB and OMP25

425   (38, 55-58). Since the upregulation of FBXO22 by *Brucella* induced the NF-κB activation and

426   production of pro-inflammatory cytokines, we speculated that FBXO22 may be nullifying the

19

427   effect of anti-inflammatory proteins of *Brucella*. We examined the effect of FBXO22 on TcpB

428   protein in-detail and demonstrated a positive interaction between FBXO22 and TcpB. The TcpB

429   effector is known to suppress NF-κB and pro-inflammatory cytokine secretion mediated by

430   TLR2/4 by promoting targeted degradation of their adaptor protein, TIRAP (56, 57). TcpB is

431   translocated into the host cells through Type IV secretory system, where it plays a key role in

432   modulating the host immune responses and endosomal trafficking for creating a replicative niche

433   in ER derived membrane vesicles (59). We found that FBXO22 could efficiently induce the

434   ubiquitination and degradation of TcpB. siRNA mediated down regulation of FBXO22 or SKP1

435   affected the degradation of TcpB that confirms the role of FBXO22 and the SCF complex for

436   degradation of TcpB. Further, we demonstrated degradation of OMP25 and Bsp1 by FBXO22.

437   Interestingly, β-TrCP did not induce degradation of any *Brucella* proteins that we tested. Studies

438   have shown that β-TrCP is upregulated   in many cancers (60). However, we did not observe

439   induction of β-TrCP in the *Brucella*-infected macrophages. These observations imply that β-

440   TrCP functions are limited to the NF-κB signaling pathways whereas FBXO22 detects the

441   *Brucella* effector proteins in the cells and direct them for degradation. Therefore, it can be

442   speculated that FBXO22 may contribute to the host defense by eliminating bacterial virulence

443   proteins. This may neutralize the impact of FBXO22-mediated enhanced invasion of intracellular

444   bacterial pathogens. Further experiments are required to address how FBXO22 drives the

445   degradation of both host and bacterial proteins through SCF complex and the molecular

446   mechanism behind the promiscuity of this F-box protein. The FBXO22 mediated degradation of

447   TcpB and OMP25 may enable host to nullify the anti-inflammatory effects of *Brucella* effector

448   proteins to establish the protective responses such as activation of NF-κB and production of

449   inflammatory cytokines.

450   In conclusion, our experimental data reveals that the host protein FBXO22 plays an essential role

451   in the uptake of *Brucella* into macrophages. FBXO22 expression is upregulated in *Brucella*

452   infected macrophages that resulted enhanced production of pro-inflammatory cytokines that may

453   contribute to the pathogenesis of brucellosis. We have also demonstrated degradation of *Brucella*

454   effector protein by FBXO22 through SCF complex, which may counteract the enhanced uptake

455   of bacterial pathogens like *Brucella,* (Fig. 8) which resist intracellular killing and survive inside

456   the cells. Our experimental data reveals the role of FBXO22 in host-pathogen interaction and in

457   the induction of pro-inflammatory responses that may contributes to the pathogenesis of

458   infectious diseases. These information may help to develop improved therapeutic strategies for

459   blocking cell invasion of microbial pathogens and for treating inflammatory disorders resulting

460   from the aberrant activation various PRRs by microbial pathogens.

Materials and Methods

461

Cell culture

462

463   Human Embryonic Kidney (HEK) 293T cells (American Type Culture Collection, ATCC),

464   murine macrophage cell line, RAW264.7 (ATCC) and immortalized Bone Marrow Derived

465   Macrophages from mouse (iBMDM; a gift from Petr Broz, University of Lausanne) were

466   cultured in Dulbecco's Modified Eagle's Medium (DMEM; Sigma) supplemented with 10% fetal

467   bovine serum (Sigma) and 1X penicillin-streptomycin solution (Gibco). RPMI 1640 medium

468   (Sigma) supplemented with 10% fetal bovine serum and 1X penicillin-streptomycin solution was

469   used to culture the murine macrophage cell line, J774 (ATCC). The cells were grown in a

470   humidified atmosphere of 5% CO_2 at 37° C. The iBMDMs were differentiated using m-CSF (20

471   ng/ml) or the culture supernatant of L929 cells (ATCC).

Silencing and overexpression of FBXO22 and other genes

472

473   The endogenous FBXO22 was silenced in murine macrophages or HEK293 cells using ON-

474   TARGETplus siRNA (Dharmacon) where the FBXO22 mRNA was targeted by a set of 4

475   siRNAs (Table 1). To silence FBXO22 in macrophages, J774 cells were seeded into 12 or 48-

476   well plate in RPMI 1640 medium supplemented with 10% FBS with antibiotics and allowed to

477   adhere overnight. The cells were then transfected with 50 pico moles of siFBXO22 or non-

478   targeting siRNA (Dharmacon) using Dharamafect-4 (Dharmacon) transfection reagent as per

479   manufacture's protocol. Forty-eight hours post-transfection, cells were lysed for immunoblotting

480   and analysed the level of FBXO22 by immunoblotting or qRT-PCR. The membrane was probed

481   with anti-FBXO22 antibody (Thermo Fisher Scientific) to detect the endogenous FBXO22. To

482   analyse the silencing of FBXO22 by qRT-PCR, total RNA was extracted from the transfected

483   cells, followed by cDNA synthesis and qRT-PCR analysis using FBXO22 specific primers

484   (Table 2).

485   To overexpress FBXO22, J774 or iBMDMs (0.5×10^5) cells were seeded into 24-well plates and

486   allowed to adhere overnight. Next, the cells were transfected with eukaryotic expression plasmid

487   harbouring FLAG or MYC-tagged FBXO22 using Xfect (TAKARA Bio) transfection reagent

488   according to manufacturer's instructions. Twenty-four hours post-transfection, cells were lysed

489   in RIPA buffer and analysed by immunoblotting. The membrane was probed with anti-FLAG

490   (Sigma) or anti-MYC (Sigma) or anti-FBXO22 antibody to detect the overexpressed protein. To

491   analyse the overexpression of FBXO22 by qRT-PCR, total RNA was extracted from transfected

492   cells, followed by cDNA synthesis and qRT-PCR analysis using FBXO22 specific primers

493   (Table 1). Data were normalized with the endogenous control, GAPDH.

494

495 **Table 1. Sequence of siRNA and CRISPR oligonucleotides.**

1	Mouse-FBXO22 siRNA	5'-GUCAGCACUUUCAGCGAUA-3' 5'-GGGAUCAGGUAGCAAUCGA-3' 5'-GAAUUUAACACUCGAAAGA-3' 5'-GGAGAUGUAAUGAGGUAAA-3'
2	FBXO22 gRNA set1	Oligo-1-5'CACCGTGTAGGGCCTTCGGGCCGGTAGG-3' Oligo-2-5'-AAACCCCTACCGGCCCGAAGGCCCTACA-3'
3	FBXO22 gRNA set2	Oligo-1-5'-CACCGTTCCTCGCCTACCGGCCCGAAGG-3' Oligo-2-5'-AAACCCCTTCGGGCCGGTAGGCGAGGAA-3'
4	FBXO22 gRNA set3	Oligo-1-5'-CACCGTTGCAGCCGGCTTAAACGCCAGG-3' Oligo-2-5'-AAACCCCTGGCGTTTAAGCCGGCTGCAA-3'
5	FBXO22 gRNA set4	Oligo-1-5'-CACCGTTCCGCCCGGAAGGGACCGGAGG-3' Oligo-2-5-AAACCCCTCCGGTCCCTTCCGGGCGGAA-3'
6	Human-FBXO22 siRNA	5'-GCACCUUCGUGUUGAGUAA-3' 5'-GGUGGGAGCCAGUAAUUAU-3' 5'-GUUCGCAUCUUACCACAUA-3' 5'-GCUUAUGGAGGGAGUGUGU-3'
7	Scrambled siRNA (NT)	5'-UUCUCCGAACGUGUCACGUTT-3'

496

Knock down of FBXO22 using CRISPR/dCas9 system

497

498 The transcriptional suppression of FBXO22 gene was performed using the CRISPR/dCas9

499 system. The Transcription Start Site (TSS) of FBXO22 gene was predicted using the DataBase

500 for Transcription Start Sites (DBTSS)(61). Subsequently, four gRNAs targeting the TSS of

501 FBXO22 gene were designed and the corresponding oligonucleotides were synthesised (Table

502 1). Next, the sense and anti-sense oligonucleotides for each gRNA were annealed and ligated

503 into BsaI digested pX601-AAV-CMV plasmid (a gift from Feng Zhang; Addgene Plasmid

504 #61591) to insert the gRNA under the U6 promoter. Next, the region that contains the CRISPR

505 elements with gRNA under U6 promoter was amplified from pX601-AAV-CMV-FBXO and

506 cloned into the PacI site of pLV hUbC-dSaCas9-KRAB-T2A-PuroR (a gift from Charles

507 Gersbach; Addgene Plasmid # 106249). The resulting FBXO22 gRNA constructs harbored the

508 gRNA1/2/3/4 with other CRISPR elements and a truncated Cas9, which lacks DNA nickase

23

509   activity (dCas9). The integrity of the plasmid constructs was confirmed by sequencing. For

510   analyzing the efficiency of FBXO22 gRNA constructs to suppress the expression of FBXO22

511   gene, J774 macrophages were seeded into 12 or 24-well plates in RPMI 1640 medium

512   supplemented with 10% FBS with antibiotics and allowed to adhere overnight. Next, the cells

513   were transfected with FBXO22 gRNA expression plasmids using X-fect transfection reagent

514   according to manufacturer's protocol. Twenty-four hours post-transfection, cells were lysed in

515   RIPA buffer and analyzed by immunoblotting using anti-FBXO22 antibody (Thermo Fisher

516   Scientific). To analyze the suppression of FBXO22 by qRT-PCR, total RNA was extracted from

517   the cells, followed by cDNA synthesis and qRT-PCR analysis. Subsequently, the gRNA

518   construct that exhibited maximum suppression of FBXO22 was selected for further analysis.

519   **Quantitative RT-PCR analysis of gene expression**

520   For analyzing the *Brucella*-induced expression of various genes by qRT-PCR, J774 or iBMDMs

521   were seeded into 24-well plates (50,000 cells/well) in RPMI medium supplemented with 10%

522   FBS without antibiotics and incubated overnight at 37° C with 5% CO2. The cells were infected

523   with *B. Neotomae* (MOI of 1000), followed by harvesting the cells at various time points. The

524   total RNA was isolated from the infected macrophages using RNAiso PLUS (Takara), followed

525   by preparation of cDNA using Prime Script™ RT Reagent kit (TAKARA) as per manufacture

526   protocol. The qRT-PCR was performed using gene specific primers (Table 1). The relative gene

527   expression was analyzed by the comparative $2^{-\Delta \Delta Ct}$ method using ABI 7500 software (Applied

528   Biosystems) or CFX 96 (BIO-RAD). Data were normalized with the endogenous control,

529   GAPDH. For analysing downregulation of target genes by siRNA or CRISPR/dCas9 system, the

530   transfected cells were harvested at 24 or 48 hours post-transfection, followed by RNA isolation,

531   cDNA preparation and qRT-PCR analysis. For analyzing the LPS-induced expression of F-box

24

532   proteins, the macrophages were treated with LPS (100 ng/ml), followed by collection of cells at

533   various time points and gene expression analysis as mentioned before. For analyzing the effect of

534   BAY 11-7082 on expression of scavenger receptors, iBMDM cells were treated with BAY 11-

535   7082 for 2 hours, followed by gene expression analysis. All the primers used for analyzing the

536   expression by qRT-PCR are listed in Table 2

537   **Table 2. List of primers used for qRT-PCR**

Serial No.	Gene	Primer sequence
1	Mouse-GAPDH	F-5'-AACGACCCCTTCATTGAC-3' R-5'-CCACGACATACTCAGCAC-3'
2	Mouse-FBXO22	F-5'-GTGGGAGCCAGTAATTACCTG-3' R-5'-GGCATCAATATCCAGAGGGTTC-3'
3	Mouse-Dectin-1	F-5'-CCAGCTAGGTGCTCATCTACTG-3' R-5'-CCTTCACTCTGATTGCGGGAAAG-3'
4	Mouse-DC-SIGN	F-5'-GCACTCCATCAAAGGCTTTGGC-3' R-5'-CAAACAGCTAGGAAGAGCACCTG-3'
5	Mouse-CD36	F-5'-GGACATTGAGATTCTTTTCCTCTG-3' R-5'-GCAAAGGCATTGGCTGGAAGAAC-3'
6	Mouse-PrPc	F-5'-CAGCAACCAGAACAACTTCGTGC-3' R-5'-CGCTCCATCATCTTCACATCGG-3'
7	Mouse-MSR1	F-5'-CGCACGTTCAATGACAGCATCC-3' R-5'-GCAAACACAAGGAGGTAGAGAGC-3'
8	Mouse-TNF-α	F-5'-GACGTGGAAGTGGCAGAAGAG-3' R-5'-TGCCACAAGCAGGAATGAGA-3'
9	Mouse-IL-6	F-5'-TCCAGTTGCCTTCTTGGGAC-3' R-5'-GTACTCCAGAAGACCAGAGG-3'
10	Human-FBXO22	F-5'-CGGAGCACCTTCGTGTTGA-3' R-5'-CACACACTCCCTCCATAAGCG-3'
11	Human-SKP1	F-5'-GACCATGTTGGAAGATTTGGGA-3' R-5'-TGCACCACTGAATGACCTTTT-3'
12	Human- GAPDH	F-5'-AATCCCATCACCATCTTCCA-3' R-5'-TGGACTCCACGACGTACTCA-3'

538

539   **Immunoblotting**

540   The harvested cells were lysed in RIPA buffer with protease inhibitor cocktail (Pierce). The

541   amount of total protein in the samples were quantified using the Bradford assay (Sigma). An

542   equal concentration of protein samples was mixed with 2X Laemmli buffer and the samples were

543   boiled for 10 min at 100°C. Next, the protein samples were run on SDS PAGE gel, followed by

544   transfer of protein onto PVDF membrane using a wet tank blotting system (Bio-Rad). The

545   membrane was blocked with 5% skimmed milk in TBST (Cell Signaling Technology) for 1 hour,

546   followed by incubation with respective primary antibody overnight at 4°C. Next, the membrane

547   was washed 3 times with TBST and incubated with HRP-conjugated secondary antibody. The

548   primary or secondary antibody was diluted in 5% skimmed milk in TBST. Finally, the membrane

549   was washed 3 times with TBST and incubated with Super Signal West Pico or Femto

550   chemiluminescent substrate (Pierce). The signals were captured using a chemi-documentation

551   system (Syngene). Antibody dilution used are listed in table 3.

552   **Table 3. Details of antibodies used for the studies**

Serial No	Antibody	Make	Dilution
1	anti-FLAG HRP-conjugated	Sigma	1:5000
2	anti-MYC HRP-conjugated	Sigma	1:5000
3	anti-HA HRP-conjugated	Sigma	1:5000
4	anti-FBXO22	Thermo	1:1000
5	anti IκBα	Cell Signalling Technology	1:1000
6	anti-Actin HRP	Sigma	1:25,000
7	anti-rabbit HRP-conjugated antibody	Cell Signalling Technology	1:5000
8	anti-mouse HRP antibody	Cell Signalling Technology	1:5000
9	anti-calreticulin	Invitrogen	1:200
10	anti- rabbit IgG alexa Fluor 647	Cell Signalling Technology	1:500

553

554

26

Infection of macrophages with *B. neotomae* or *B. melitensis*

555

556   The macrophages were plated in multi-well plates and allowed to adhere overnight. The cells

557   were then infected at a multiplicity of infection (MOI) 1000:1 and 200:1 for *B. neotomae* and *B.*

558   *melitensis* respectively. After adding *Brucella,* the plates were centrifuged at 280 x g for 3

559   minutes to pellet-down the bacteria onto the cell. Subsequently, the plates were incubated for 90

560   minutes at 37° C with 5% CO_2. Next, the cells were washed three times with phosphate-buffered

561   saline (PBS) and treated with 30 µg/ml gentamicin for 30 minutes to kill extracellular *Brucella*.

562   The infected cells were lysed with 0.1% Triton X-100 in PBS at various hours post-infection,

563   followed by serial dilution of lysates and plating on *brucella* agar (BD). Intracellular *Brucella*

564   was quantified by enumerating the Colony Forming Units (CFU) and represented as CFU/ml.

565   For invasion assay, *B. neotomae* or *B. melitensis* was added into the multi-well plates harboring

566   macrophages, followed by pelleting down the bacteria onto the cells by centrifugation.

567   Subsequently, the plates were incubated for 30, 60 or 90 minutes at 37° C with 5% CO_2. Next,

568   the cells were the washed three times with PBS and treated with 30 µg/ml gentamicin for 30

569   minutes to kill extracellular *Brucella*. Subsequently, the infected cells were lysed with 0.1%

570   Triton X-100 in PBS, followed by serial dilution of lysates and plating on brucella agar. The

571   intracellular *Brucella* was quantified by enumerating the Colony Forming Units (CFU/ml).

572   For infecting the FBXO22 knock-down macrophages, cells were transfected with siRNA (50

573   pico mol) and CRISPR-dCas9 harboring gRNA of FBXO22 (500 ng) for 48 hours and 24 hours

574   respectively, followed by infection with *Brucella* as mentioned before. To infect macrophages

575   overexpressing F-box proteins, cells were transfected with Empty vector (EV) or pcDNA-FLAG-

576   FBXO22 or pcDNA-FLAG- β-TrcP, followed by infection with *B. neotomae* or *B. melitensis*, 24

577   hours post-infection. To perform macrophage infection in presence of NF-κB inhibitor, cells

27

578   were treated with BAY 11-7082 or DMSO (vehicle) at a concentration of 10 μM for 1 hour,

579   followed by infection with *Brucella.* BAY 11-7082 or DMSO was maintained in the media

580   throughout the time of infection. For performing *Brucella* invasion assay in the presence of BAY

581   11-7082 in the FBXO22 overexpressing macrophages, cells were transfected with MYC-

582   FBXO22. Twenty-four hours post-transfection, the cells were treated with BAY 11-7082 or

583   DMSO (vehicle) at a concentration of 10 μM for 1 hour, followed by infection with *Brucella.*

584   To perform re-infection study, iBMDMs were plated in 24-well plates and allowed to adhere

585   overnight. Next, *B. neotomae or B. neotomae*-GFP was added into the wells, followed by

586   pelleting down the bacteria by centrifugation. Subsequently, the plates were incubated for 90

587   minutes at 37°C with 5% $CO_2.$ The cells were then washed three times with PBS and treated

588   with gentamicin (30 µg/ml) for 30 minutes to kill extracellular *Brucella*. After 2 or 4 hours of

589   primary infection, the cells were re-infected with *B. neotomae* or *B. neotomae*-tdTomato for 30

590   minutes, followed by gentamycin treatment to kill extracellular *Brucella.* The number of invaded

591   *B. neotomae* and *B. neotomae*-tdTomato were quantified by enumerating CFU and by fluorescent

592   microscopy, respectively.

593   **Confocal and Immunofluorescence microscopy**

594   In order to generate *B. neotomae* expressing fluorescent protein, plasmid constructs expressing

595   GFP or tdTomato (Red) (a kind gift from Gary Splitter, University of Wisconsin-Madison) were

596   electroporated into *B. neotomae* using a micropulser (Biorad). The transformants were selected

597   on *Brucella* agar containing chloramphenicol (40 mg/ml). To perform confocal microscopy

598   analysis, the *Brucella*-infected macrophages were washed with PBS and fixed with 4% para-

599   formaldehyde for 20 minutes. The cells were permeabilized with 0.1% Triton X 100 in PBS for

600   10 min. Subsequently, the cells were blocked with 1% BSA in PBS containing 50 mM NH_4Cl

28

601   for 30 min. The cells were then incubated with anti-calreticulin antibody for 1 hour, followed by

602   Alexa Fluor-647-conjugated secondary antibody to stain endoplasmic reticulum. Finally, the

603   cells were mounted in Prolong Gold anti-fading agent with DAPI (Thermo Fisher Scientific).

604   The cells were analyzed using a laser confocal microscope at 40X magnification (Leica). For

605   fluorescent microscopy, the infected cells were fixed with 4 % paraformaldehyde in PBS,

606   followed by staining the nucleus with Hoechst (Thermo Fisher Scientific). The images were

607   captured using a florescent microscope (Carl Zeiss) at 20 X magnification.

608   **NF-κB luciferase reporter assay**

609   RAW 264 cells were seeded into 24-well plates (50,000 cells/well) in DMEM medium

610   supplemented with 10% FBS without antibiotics and incubated overnight at 37° C with 5% CO_2.

611   Cells were then transfected with pLuc-NF-κB (50 ng/well) and pRL-TK (100 ng/well) using X-

612   fect transfection reagent according to manufacturer's instructions. Twelve hours post-

613   transfections, cells were infected with *B. neotomae* (MOI 1:1000) and the cells were harvested at

614   various time points. Cells were then lysed with 1X passive lysis buffer at 4° C for 30 minutes,

615   followed by quantification of expression levels of Firefly and Renilla luciferase using Dual

616   Luciferase Reporter Assay System (Promega). The data was expressed as fold change of NF-κB

617   activation in infected *vs* uninfected cells for each time point.

618   **Cytokine analysis**

619   The secreted TNF-α and IL-6 cytokines in the culture supernatants were quantified by ELISA

620   using Duo Set ELISA (R&D systems) as per the manufactures instructions. The expression

621   levels of TNF-α and IL-6 in macrophages were quantified by qRT-PCR using the cytokine

622   specific primers as described before. For analyzing the TNF-α levels in BAY 11-7082 treated

623   cells, iBMDM were treated with BAY 11-7082 for 1 hour, followed by infection with various

29

624   MOI of *B. neotomae*. The cells were then harvested, followed by quantification of TNF-α

625   expression by qRT-PCR. Primers used are listed in Table 2.

Co-immunoprecipitation

627   HEK293T cells (0.3 X10^6) were transfected with pCMV-FLAG-FBXO22 using Turbofect

628   (Thermo Fisher) in 6-well plate. Twenty-four hours after transfection, cells were lysed at 4°C in

629   cell lysis buffer containing 20 mM Tris (pH 8.0), 150 mM NaCl, 1% Triton X-100, 1 mM

630   EDTA, and 1X protease inhibitor cocktail, followed by clarification of the lysate by

631   centrifugation at 12,000 rpm for 20 min. To determine the interaction between TcpB and

632   FBXO22, the above lysate was mixed with purified MBP-TcpB fusion protein or MBP alone.

633   The lysates were precleared with Protein G Plus-agarose beads (Santa Cruz Biotechnology) and

634   mixed with 5 µg of anti-FLAG antibody (Sigma) and incubated overnight at 4° C on a rotator.

635   Next, Protein G Plus-agarose was added to the samples and incubated for 3 hours at 4° C on a

636   rotator. Subsequently, the beads were washed three times with TNT buffer (20 mM Tris (pH8.0),

637   150 mM NaCl, and 1% Triton X-100) and resuspended in 30 µl of SDS sample buffer (Bio-Rad)

638   and boiled for 10 minutes, followed by SDS-PAGE and immunoblotting. The membrane was

639   probed with horseradish peroxidase (HRP)-conjugated anti-MBP antibody (NEB) and HRP-

640   conjugated anti-FLAG antibody to detect MBP-TcpB and FBXO22, respectively.

Co-transfection and protein degradation experiments

642   HEK293T cells (0.1 x 10^6) were co-transfected with 300 ng of either pCMV-HA-TcpB/Omp25d

643   (Accession JQ839278) or pcDNA-FLAG-BspI and increasing concentrations (300 ng, 600 ng,

644   900 ng, and 1.2 µg) of either FLAG or MYC-tagged FBXO22 or MYC-β-TrCp in a 12-well

645   plate. To check the degradation of TcpB with FBXO22 in presence of GogB, cells were co-

646   transfected with 300 ng of pCMV-HA-TcpB, 900 ng of pCMV-MYC-FBXO22 and 300 ng

30

647   pcDNA-FLAG-GogB of in a 12-well plate. Twenty-four hours after transfection, the cells were

648   lysed in RIPA buffer, followed by immunoblotting as described before. The membranes were

649   probed with respective HRP-conjugated primary antibodies against the tags.

650   For checking levels of TcpB in FBXO22 or SKP1 silenced cells, HEK293T cells were seeded

651   into 12-well plates (0.1 $X10^6$ cells/well) in complete DMEM medium and incubated overnight at

652   37° C with 5% CO_2. Cells were then transfected with non-targeting (NT) siRNA or siRNA

653   specific for human FBXO22 or SKP1 (50 pmol) using Dharamafect-4 (Dharmacon) transfection

654   reagent. Twenty-four-hour post-transfection, cells were re-transfected with 300 ng of pCMV-

655   HA-TcpB. Twenty-four hours after pCMV-HA-TcpB transfection, cells were lysed and

656   subjected to immunoblotting. The membrane was probed with HRP-conjugated anti-HA

657   antibody to detect HA-tagged TcpB.

658

659   To check the TcpB levels in *Salmonella* infected cells, HEK293T cells were seeded into 12-well

660   plates (0.1 $X10^6$ cells/well) in complete DMEM medium without antibiotics and incubated

661   overnight at 37° C with 5% CO_2. Cells were the co-transfected with 300 ng pCMV-HA-TcpB

662   and 900 ng of MYC-FBXO22. *S. enterica Typhimurium* (ATCC 14028) was cultured in LB

663   broth (HiMedia) overnight at 37 °C. Three hours before the infection, the *Salmonella* culture was

664   diluted (1:50) with fresh LB broth containing 300 mM NaCl and grown without shaking for 3

665   hours at

666   37° C, followed by harvesting the bacteria. Subsequently, the transfected HEK293 cells were

667   infected for 90 minutes, followed by treatment with gentamicin (100 µg/ml) to kill the

668   extracellular bacteria and the cells were maintained at 50 µg/ml gentamycin. Twenty four hours

31

669   post-infection, the cells were lysed at 4° C in RIPA buffer and subjected to immunoblotting. The

670   membrane was probed with HRP-conjugated anti-HA antibody to detect HA-tagged TcpB.

671   *In vivo* **ubiquitination assays**

672   HEK293T cells ($0.3X10^6$) were co-transected with 1.5 μg of pCMV-FLAG-TcpB, 1.5 μg of

673   pCMV-MYC-FBXO22, and 1 μg of pCMV-HA-ubiquitin. Total DNA concentration was

674   maintained at 4 μg using empty vector. Twenty-four hours after transfection, cells were washed

675   with PBS and lysed in 400 μl of lysis buffer containing 20 mM Tris-HCI (pH 7.4) and 1% SDS

676   (24). Cell lysates were boiled for 10 minutes and clarified by centrifugation at 13,000 rpm for 15

677   min. Subsequently, the cell lysates were diluted with buffer containing 20 mM Tris-HCl (pH

678   7.5), 150 mM NaCl, 2% Triton X-100, and 0.5% Nonidet P-40(57).Next, 5μg of anti-FLAG

679   antibody was added to the lysates and incubated overnight at 4° C on rotator.

680   Immunoprecipitation and immunoblotting were performed with samples as described above. The

681   membrane was probed with HRP-conjugated anti-HA and anti-FLAG antibodies to detect HA-

682   ubiquitin and FLAG-TcpB, respectively. FBXO22 was detected in whole-cell lysate using HRP-

683   conjugated anti-MYC antibody (Sigma).

684   **Statistical analysis**

685   The GraphPad Prism 6.0 software was for statistical analysis of experimental data. Data are

686   shown as mean ± SEM. Statistical significance was determined by t tests (two-tailed).

687   **Acknowledgments**

694

References

696

697 1.   Pappas G, Akritidis N, Bosilkovski M, Tsianos E. Brucellosis. The New England journal
698 of medicine. 2005;352(22):2325-36.
699 2.   Pappas G, Panagopoulou P, Christou L, Akritidis N. Brucella as a biological weapon.
700 Cellular and molecular life sciences : CMLS. 2006;63(19-20):2229-36.
701 3.   Bukhari EE. Pediatric brucellosis. An update review for the new millennium. Saudi
702 medical journal. 2018;39(4):336-41.
703 4.   Ranjbar M. Treatment of Brucellosis. Updates on Brucellosis2015.
704 5.   Ariza J, Bosilkovski M, Cascio A, Colmenero JD, Corbel MJ, Falagas ME, et al.
705 Perspectives for the treatment of brucellosis in the 21st century: the Ioannina recommendations.
706 PLoS medicine. 2007;4(12):e317.
707 6.   Roop RM, 2nd, Gaines JM, Anderson ES, Caswell CC, Martin DW. Survival of the
708 fittest: how Brucella strains adapt to their intracellular niche in the host. Medical microbiology
709 and immunology. 2009;198(4):221-38.
710 7.   Pizarro-Cerdá J, Moreno E, Sanguedolce V, Mege JL, Gorvel JP. Virulent Brucella
711 abortus Prevents Lysosome Fusion and Is Distributed within Autophagosome-Like
712 Compartments. Infection and immunity. 1998;66(5):2387-92.
713 8.   Celli J. Surviving inside a macrophage: the many ways of Brucella. Research in
714 microbiology. 2006;157(2):93-8.
715 9.   Seleem MN, Boyle SM, Sriranganathan N. Brucella: a pathogen without classic virulence
716 genes. Veterinary microbiology. 2008;129(1-2):1-14.
717 10.   Qin QM, Pei J, Ancona V, Shaw BD, Ficht TA, de Figueiredo P. RNAi screen of
718 endoplasmic reticulum-associated host factors reveals a role for IRE1alpha in supporting
719 Brucella replication. PLoS pathogens. 2008;4(7):e1000110.
720 11.   Petroski MD, Deshaies RJ. Function and regulation of cullin-RING ubiquitin ligases.
721 Nature reviews Molecular cell biology. 2005;6(1):9-20.
722 12.   Xie J, Jin Y, Wang G. The role of SCF ubiquitin-ligase complex at the beginning of life.
723 Reproductive biology and endocrinology : RB&E. 2019;17(1):101.
724 13.   Zhang L, Chen J, Ning D, Liu Q, Wang C, Zhang Z, et al. FBXO22 promotes the
725 development of hepatocellular carcinoma by regulating the ubiquitination and degradation of
726 p21. Journal of experimental & clinical cancer research : CR. 2019;38(1):101.

14.   Hou XK, Mao JS. Long noncoding RNA SNHG14 promotes osteosarcoma progression via miR-433-3p/FBXO22 axis. Biochemical and biophysical research communications. 2020.

15.   Lignitto L, LeBoeuf SE, Homer H, Jiang S, Askenazi M, Karakousi TR, et al. Nrf2 Activation Promotes Lung Cancer Metastasis by Inhibiting the Degradation of Bach1. Cell. 2019;178(2):316-29.e18.

16.   Zhu XN, He P, Zhang L, Yang S, Zhang HL, Zhu D, et al. FBXO22 mediates polyubiquitination and inactivation of LKB1 to promote lung cancer cell growth. Cell death & disease. 2019;10(7):486.

17.   Zheng Y, Chen H, Zhao Y, Zhang X, Liu J, Pan Y, et al. Knockdown of FBXO22 inhibits melanoma cell migration, invasion and angiogenesis via the HIF-1alpha/VEGF pathway. Investigational new drugs. 2020;38(1):20-8.

18.   Tian X, Dai S, Sun J, Jin G, Jiang S, Meng F, et al. F-box protein FBXO22 mediates polyubiquitination and degradation of KLF4 to promote hepatocellular carcinoma progression. Oncotarget. 2015;6(26):22767-75.

19.   Sun R, Xie HY, Qian JX, Huang YN, Yang F, Zhang FL, et al. FBXO22 Possesses Both Protumorigenic and Antimetastatic Roles in Breast Cancer Progression. Cancer research. 2018;78(18):5274-86.

20.   Johmura Y, Maeda I, Suzuki N, Wu W, Goda A, Morita M, et al. Fbxo22-mediated KDM4B degradation determines selective estrogen receptor modulator activity in breast cancer. The Journal of clinical investigation. 2018;128(12):5603-19.

21.   Guo F, Liu J, Han X, Zhang X, Lin T, Wang Y, et al. FBXO22 Suppresses Metastasis in Human Renal Cell Carcinoma via Inhibiting MMP-9-Mediated Migration and Invasion and VEGF-Mediated Angiogenesis. International journal of biological sciences. 2019;15(3):647-56.

22.   Wu B, Liu ZY, Cui J, Yang XM, Jing L, Zhou Y, et al. F-Box Protein FBXO22 Mediates Polyubiquitination and Degradation of CD147 to Reverse Cisplatin Resistance of Tumor Cells. International journal of molecular sciences. 2017;18(1).

23.   Johmura Y, Sun J, Kitagawa K, Nakanishi K, Kuno T, Naiki-Ito A, et al. SCF(Fbxo22)-KDM4A targets methylated p53 for degradation and regulates senescence. Nature communications. 2016;7:10574.

24.   Pilar AV, Reid-Yu SA, Cooper CA, Mulder DT, Coombes BK. GogB is an anti-inflammatory effector that limits tissue damage during Salmonella infection through interaction with human FBXO22 and Skp1. PLoS pathogens. 2012;8(6):e1002773.

25.   Kang YS, Brown DA, Kirby JE. Brucella neotomae Recapitulates Attributes of Zoonotic Human Disease in a Murine Infection Model. Infection and immunity. 2019;87(1).

26.   Covert J, Mathison AJ, Eskra L, Banai M, Splitter G. Brucella melitensis, B. neotomae and B. ovis elicit common and distinctive macrophage defense transcriptional responses. Experimental biology and medicine (Maywood, NJ). 2009;234(12):1450-67.

27.   Rossetti CA, Drake KL, Siddavatam P, Lawhon SD, Nunes JE, Gull T, et al. Systems biology analysis of Brucella infected Peyer's patch reveals rapid invasion with modest transient perturbations of the host transcriptome. PLoS one. 2013;8(12):e81719.

28.   Huy TXN, Reyes AWB, Hop HT, Arayan LT, Son VH, Min W, et al. Emodin Successfully Inhibited Invasion of Brucella abortus Via Modulting Adherence, Microtubule Dynamics and ERK Signaling Pathway in RAW 264.7 Cells. Journal of microbiology and biotechnology. 2018;28(10):1723-9.

29.   Qi LS, Larson MH, Gilbert LA, Doudna JA, Weissman JS, Arkin AP, et al. Repurposing CRISPR as an RNA-guided platform for sequence-specific control of gene expression. Cell. 2013;152(5):1173-83.

30.   Bai J, Wu K, Cao MH, Yang Y, Pan Y, Liu H, et al. SCF(FBXO22) targets HDM2 for degradation and modulates breast cancer cell invasion and metastasis. Proceedings of the National Academy of Sciences of the United States of America. 2019;116(24):11754-63.

31.   Wong CO, Gregory S, Hu H, Chao Y, Sepúlveda VE, He Y, et al. Lysosomal Degradation Is Required for Sustained Phagocytosis of Bacteria by Macrophages. Cell host & microbe. 2017;21(6):719-30.e6.

32.   Geijtenbeek TB, van Vliet SJ, Engering A, t Hart BA, van Kooyk Y. Self- and nonself-recognition by C-type lectins on dendritic cells. Annual review of immunology. 2004;22:33-54.

33.   Peiser L, Mukhopadhyay S, Gordon S. Scavenger receptors in innate immunity. Current opinion in immunology. 2002;14(1):123-8.

34.   Taylor PR, Martinez-Pomares L, Stacey M, Lin HH, Brown GD, Gordon S. Macrophage receptors and immune recognition. Annual review of immunology. 2005;23:901-44.

35.   Underhill DM, Ozinsky A. Phagocytosis of microbes: complexity in action. Annual review of immunology. 2002;20:825-52.

36.   Watarai M, Kim S, Erdenebaatar J, Makino S, Horiuchi M, Shirahata T, et al. Cellular prion protein promotes Brucella infection into macrophages. The Journal of experimental medicine. 2003;198(1):5-17.

37.   Iyori M, Kataoka H, Shamsul HM, Kiura K, Yasuda M, Nakata T, et al. Resveratrol modulates phagocytosis of bacteria through an NF-kappaB-dependent gene program. Antimicrobial agents and chemotherapy. 2008;52(1):121-7.

38.   Luo X, Zhang X, Wu X, Yang X, Han C, Wang Z, et al. Brucella Downregulates Tumor Necrosis Factor-α to Promote Intracellular Survival via Omp25 Regulation of Different MicroRNAs in Porcine and Murine Macrophages. Frontiers in immunology. 2017;8:2013.

39.   Radhakrishnan GK, Splitter GA. Biochemical and functional analysis of TIR domain containing protein from Brucella melitensis. Biochemical and biophysical research communications. 2010;397(1):59-63.

40.   Schulman BA, Carrano AC, Jeffrey PD, Bowen Z, Kinnucan ER, Finnin MS, et al. Insights into SCF ubiquitin ligases from the structure of the Skp1-Skp2 complex. Nature. 2000;408(6810):381-6.

41.   Areschoug T, Gordon S. Scavenger receptors: role in innate immunity and microbial pathogenesis. 2009;11(8):1160-9.

805   42.   Baranova IN, Kurlander R, Bocharov AV, Vishnyakova TG, Chen Z, Remaley AT, et al.
806   Role of human CD36 in bacterial recognition, phagocytosis, and pathogen-induced JNK-
807   mediated signaling. Journal of immunology (Baltimore, Md : 1950). 2008;181(10):7147-56.
808   43.   Njiri OA, Zhang X, Zhang Y, Wu B, Jiang L, Li Q, et al. CD209 C-Type Lectins
809   Promote Host Invasion, Dissemination, and Infection of Toxoplasma gondii. Frontiers in
810   immunology. 2020;11:656.
811   44.   Zeituni AE, Jotwani R, Carrion J, Cutler CW. Targeting of DC-SIGN on human dendritic
812   cells by minor fimbriated Porphyromonas gingivalis strains elicits a distinct effector T cell
813   response. Journal of immunology (Baltimore, Md : 1950). 2009;183(9):5694-704.
814   45.   Colmenares M, Puig-Kröger A, Pello OM, Corbí AL, Rivas L. Dendritic cell (DC)-
815   specific intercellular adhesion molecule 3 (ICAM-3)-grabbing nonintegrin (DC-SIGN, CD209),
816   a C-type surface lectin in human DCs, is a receptor for Leishmania amastigotes. The Journal of
817   biological chemistry. 2002;277(39):36766-9.
818   46.   Geijtenbeek TB, Kwon DS, Torensma R, van Vliet SJ, van Duijnhoven GC, Middel J, et
819   al. DC-SIGN, a dendritic cell-specific HIV-1-binding protein that enhances trans-infection of T
820   cells. Cell. 2000;100(5):587-97.
821   47.   Cambi A, Gijzen K, de Vries l J, Torensma R, Joosten B, Adema GJ, et al. The C-type
822   lectin DC-SIGN (CD209) is an antigen-uptake receptor for Candida albicans on dendritic cells.
823   European journal of immunology. 2003;33(2):532-8.
824   48.   Geijtenbeek TB, Van Vliet SJ, Koppel EA, Sanchez-Hernandez M, Vandenbroucke-
825   Grauls CM, Appelmelk B, et al. Mycobacteria target DC-SIGN to suppress dendritic cell
826   function. The Journal of experimental medicine. 2003;197(1):7-17.
827   49.   Głowacka P, Żakowska D, Naylor K, Niemcewicz M, Bielawska-Drózd A. Brucella -
828   Virulence Factors, Pathogenesis and Treatment. Polish journal of microbiology. 2018;67(2):151-
829   61.
830   50.   Hop HT, Reyes AWB, Huy TXN, Arayan LT, Min W, Lee HJ, et al. Activation of NF-
831   kB-Mediated TNF-Induced Antimicrobial Immunity Is Required for the Efficient Brucella
832   abortus Clearance in RAW 264.7 Cells. Frontiers in cellular and infection microbiology.
833   2017;7:437.
834   51.   Kim S, Lee DS, Watanabe K, Furuoka H, Suzuki H, Watarai M. Interferon-gamma
835   promotes abortion due to Brucella infection in pregnant mice. BMC microbiology. 2005;5:22.
836   52.   Fernández AG, Hielpos MS, Ferrero MC, Fossati CA, Baldi PC. Proinflammatory
837   response of canine trophoblasts to Brucella canis infection. PloS one. 2017;12(10):e0186561.
838   53.   Gu W, Wang X, Qiu H, Cui B, Zhao S, Zheng H, et al. Comparison of cytokine immune
839   responses to Brucella abortus and Yersinia enterocolitica serotype O:9 infections in BALB/c
840   mice. Infection and immunity. 2013;81(12):4392-8.
841   54.   Liu J, Peng Y, Zhang J, Long J, Liu J, Wei W. Targeting SCF E3 Ligases for Cancer
842   Therapies. Advances in experimental medicine and biology. 2020;1217:123-46.

843   55.   Cirl C, Wieser A, Yadav M, Duerr S, Schubert S, Fischer H, et al. Subversion of Toll-like
844   receptor signaling by a unique family of bacterial Toll/interleukin-1 receptor domain-containing
845   proteins. Nature medicine. 2008;14(4):399-406.
846   56.   Radhakrishnan GK, Yu Q, Harms JS, Splitter GA. Brucella TIR Domain-containing
847   Protein Mimics Properties of the Toll-like Receptor Adaptor Protein TIRAP. The Journal of
848   biological chemistry. 2009;284(15):9892-8.
849   57.   Sengupta D, Koblansky A, Gaines J, Brown T, West AP, Zhang D, et al. Subversion of
850   innate immune responses by Brucella through the targeted degradation of the TLR signaling
851   adapter, MAL. Journal of immunology (Baltimore, Md : 1950). 2010;184(2):956-64.
852   58.   Jubier-Maurin V, Boigegrain RA, Cloeckaert A, Gross A, Alvarez-Martinez MT, Terraza
853   A, et al. Major outer membrane protein Omp25 of Brucella suis is involved in inhibition of
854   tumor necrosis factor alpha production during infection of human macrophages. Infection and
855   immunity. 2001;69(8):4823-30.
856   59.   Felix C, Kaplan Turkoz B, Ranaldi S, Koelblen T, Terradot L, O'Callaghan D, et al. The
857   Brucella TIR domain containing proteins BtpA and BtpB have a structural WxxxE motif
858   important for protection against microtubule depolymerisation. Cell communication and
859   signaling : CCS. 2014;12:53.
860   60.   Yan L, Lin M, Pan S, Assaraf YG, Wang ZW, Zhu X. Emerging roles of F-box proteins
861   in cancer drug resistance. Drug resistance updates : reviews and commentaries in antimicrobial
862   and anticancer chemotherapy. 2019;49:100673.
863   61.   Suzuki Y, Yamashita R, Nakai K, Sugano S. DBTSS: DataBase of human Transcriptional
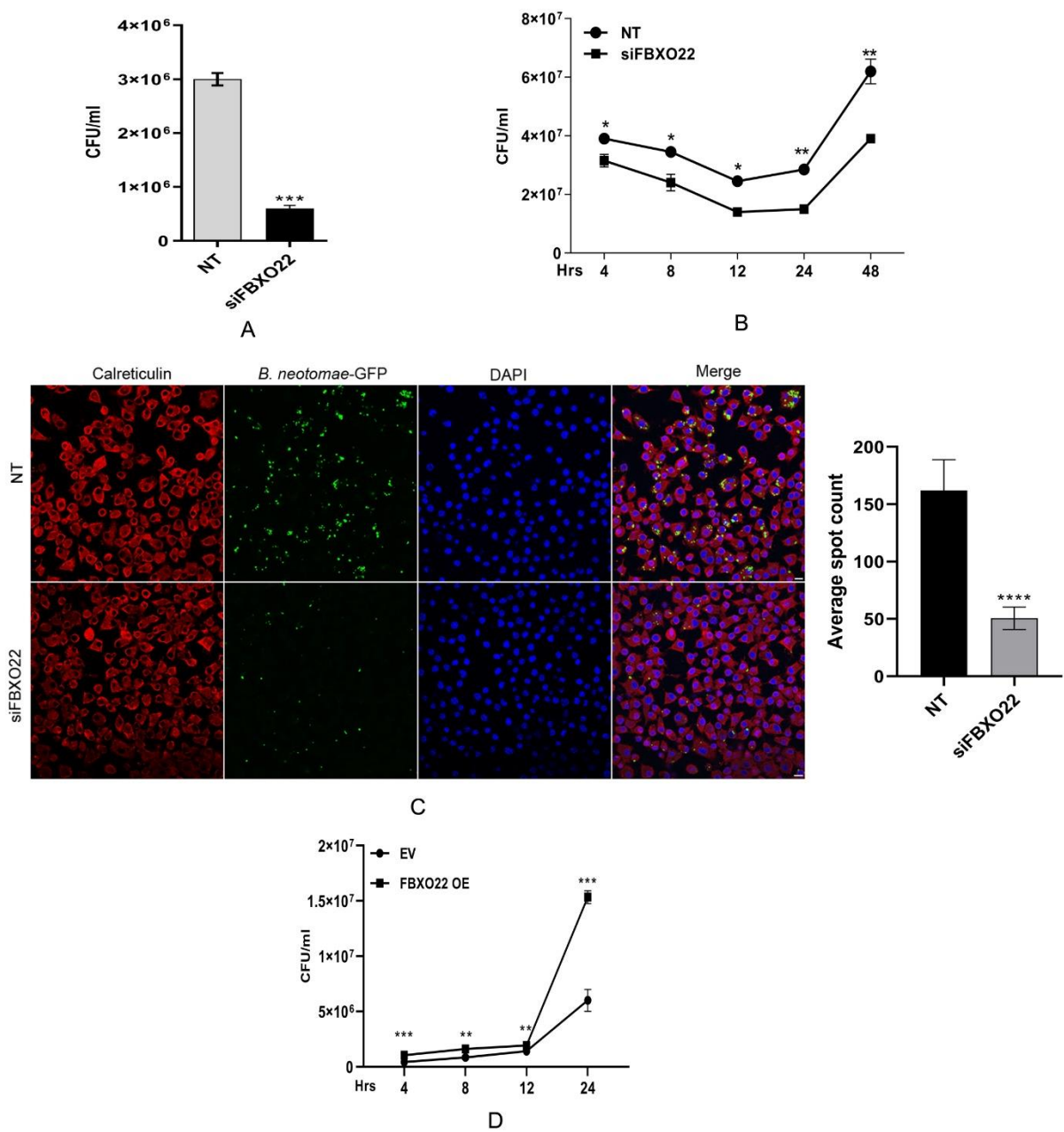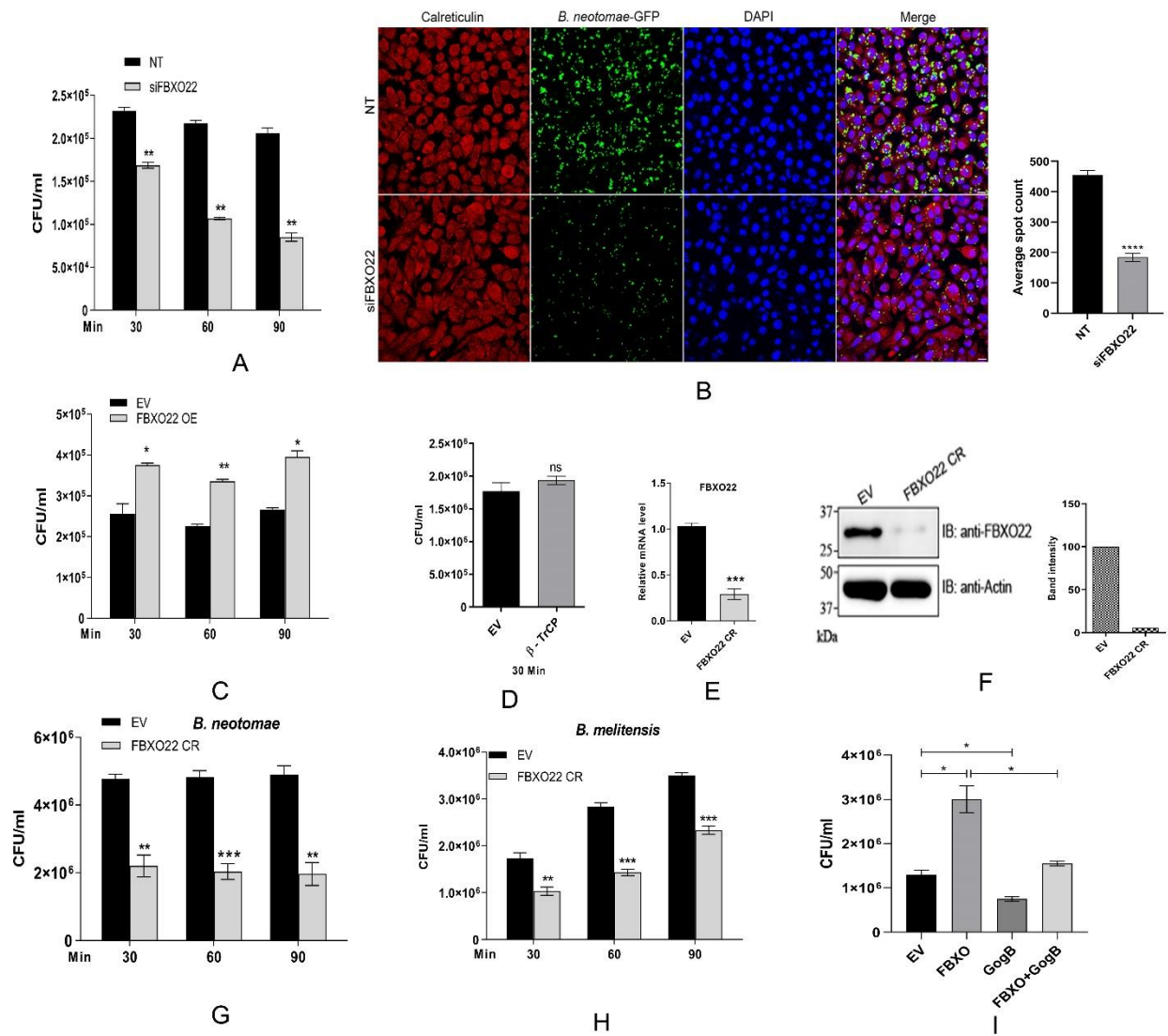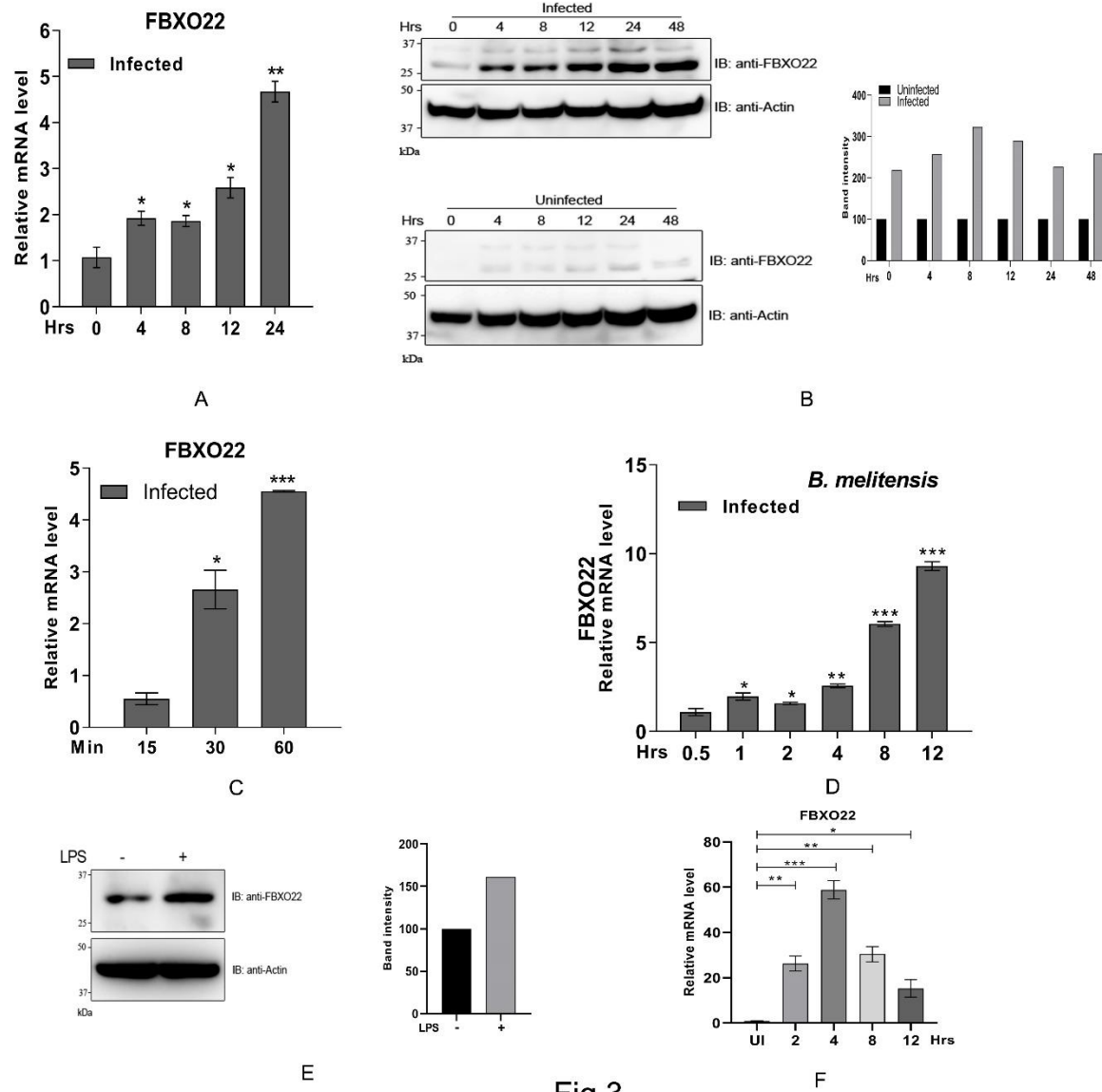864   Start Sites and full-length cDNAs. Nucleic acids research. 2002;30(1):328-31.

865

866

867

868

869

870

871

872

873

874

875

876

877 **Figures**

Fig 1

878

879

Fig 2

880

Fig 3

881

882

40

Fig 4

883

884

885

886

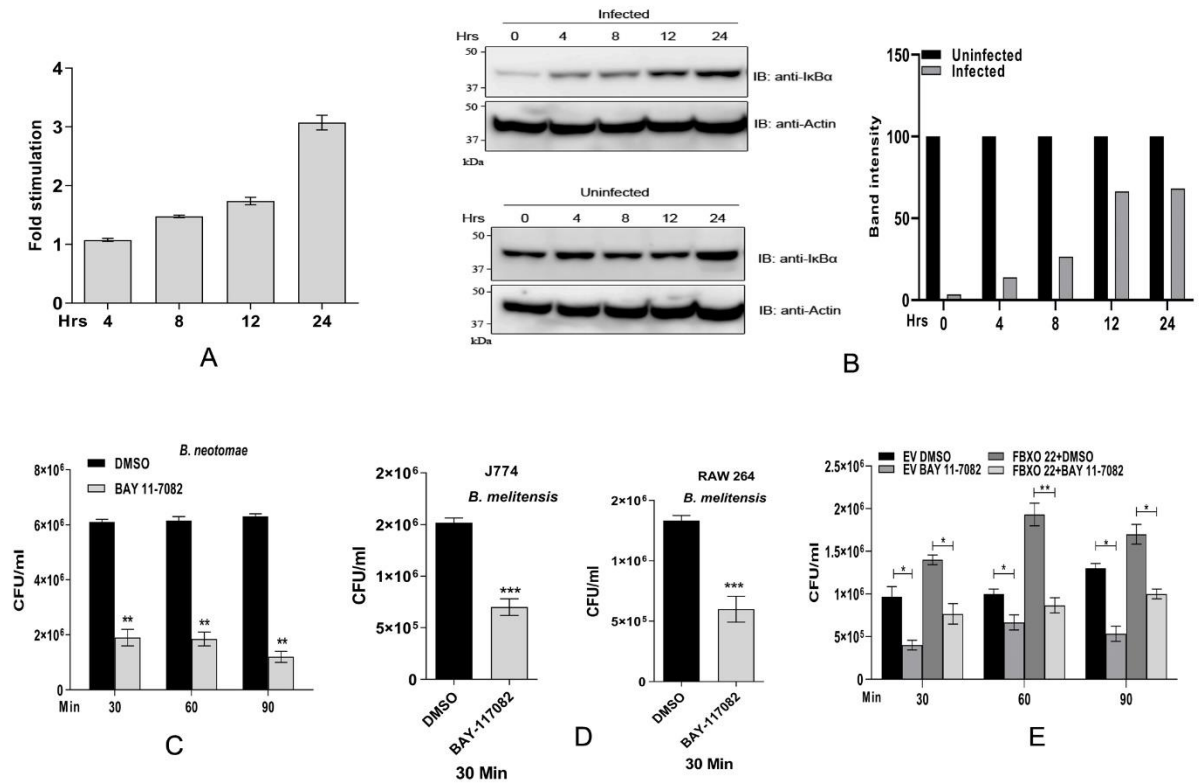887

888

889

890

891

892

893

894

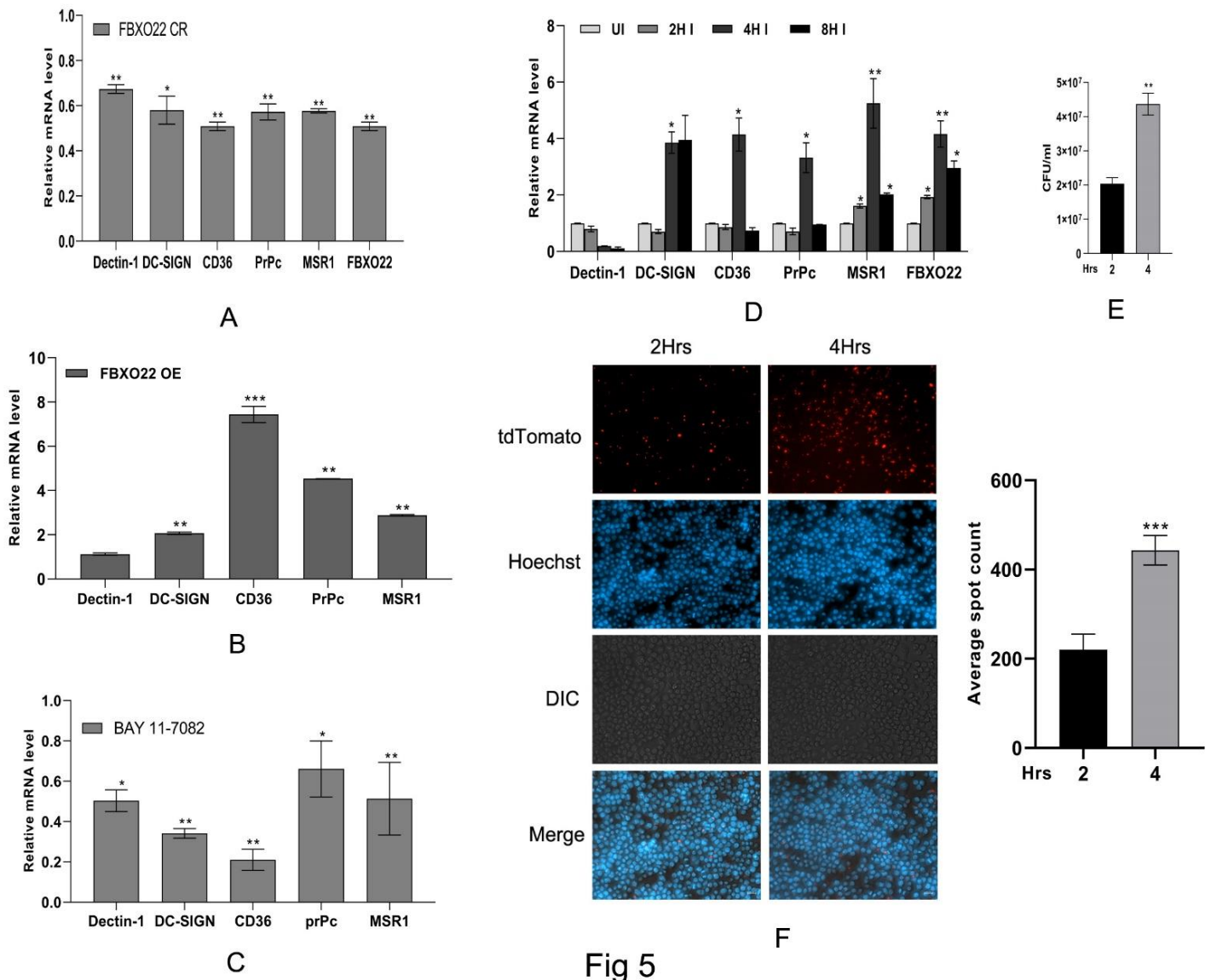895

896

897

898

899

900

Fig 5

901
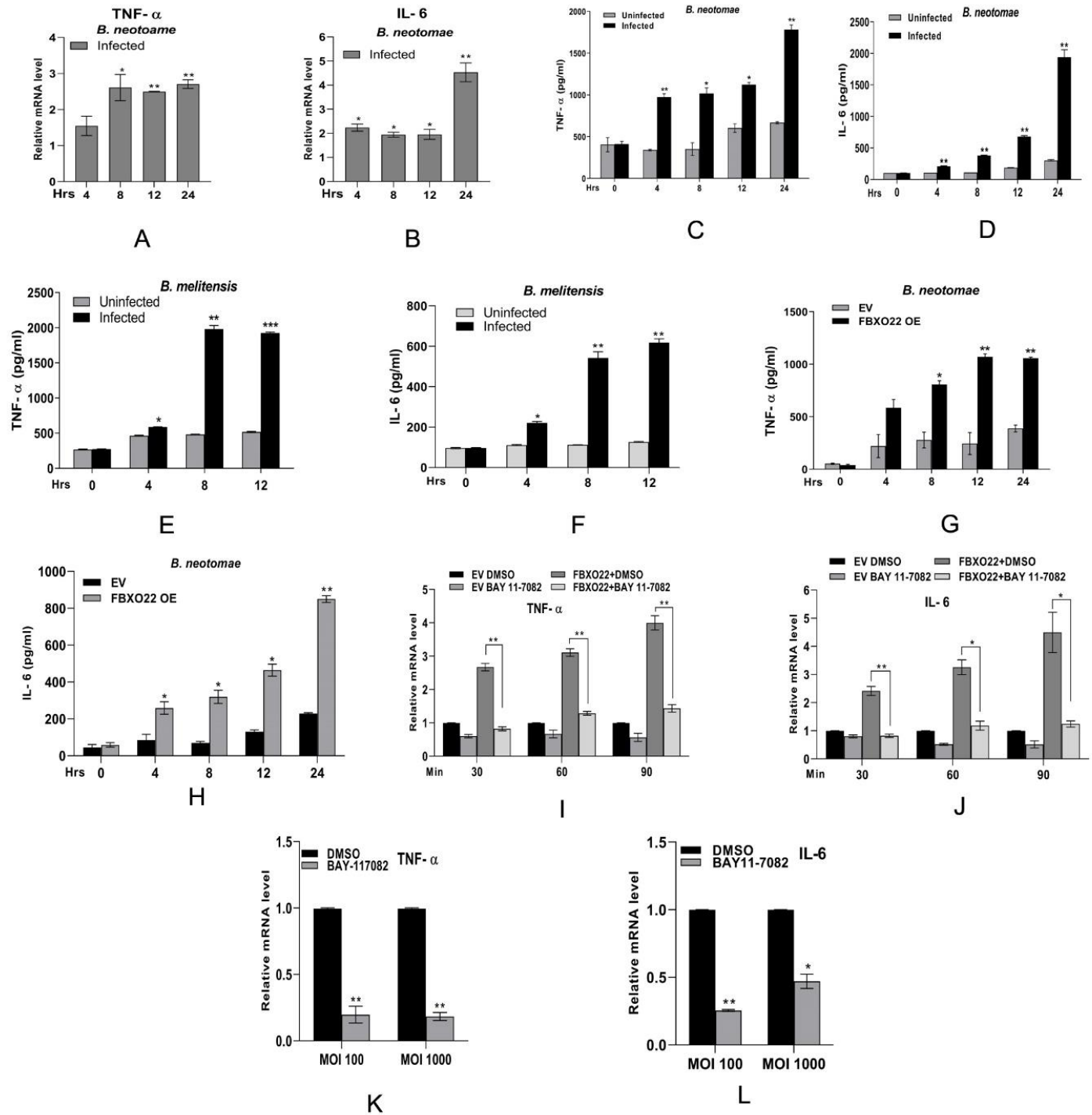
42

902
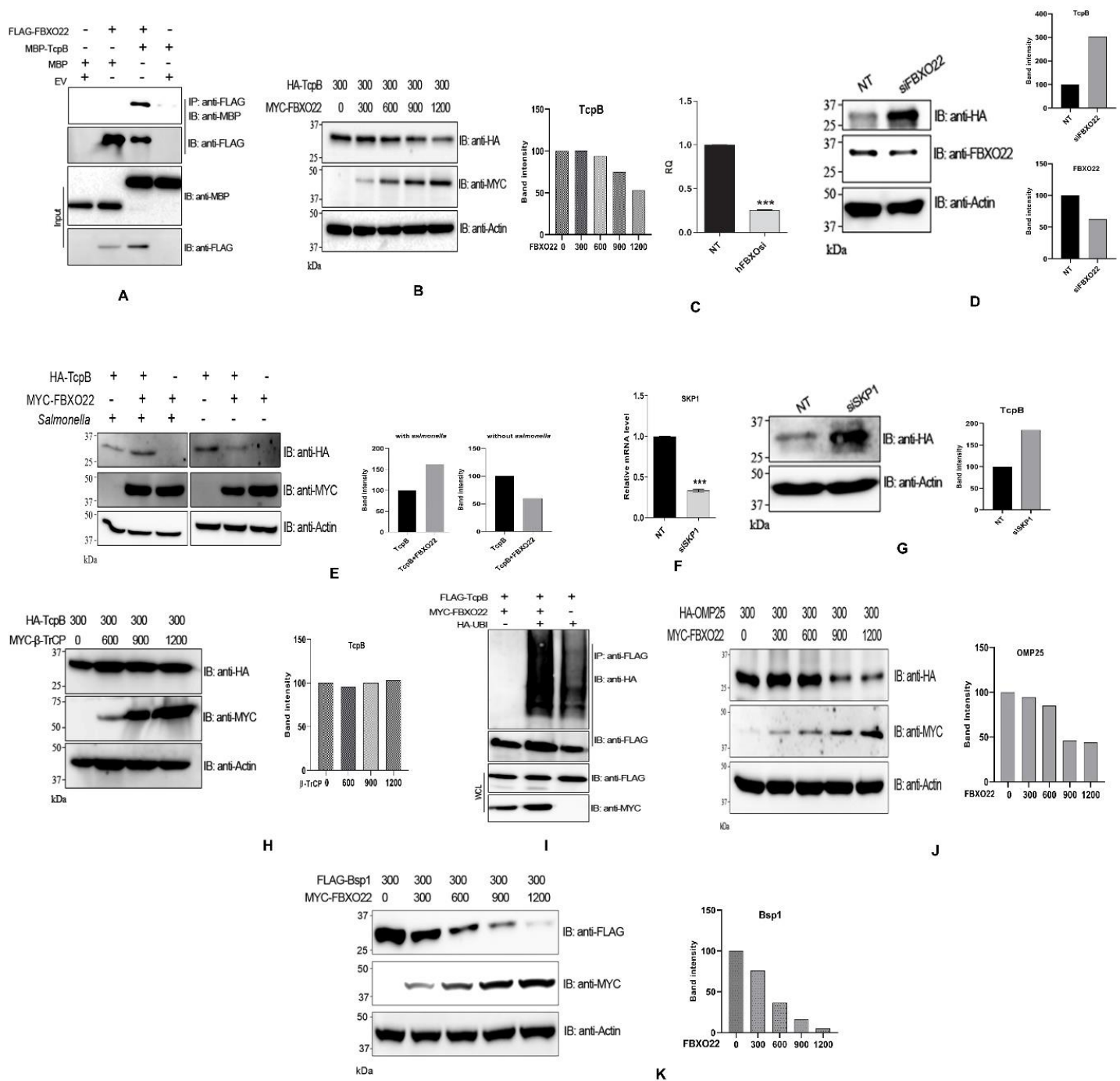
903

Fig 6

43

904

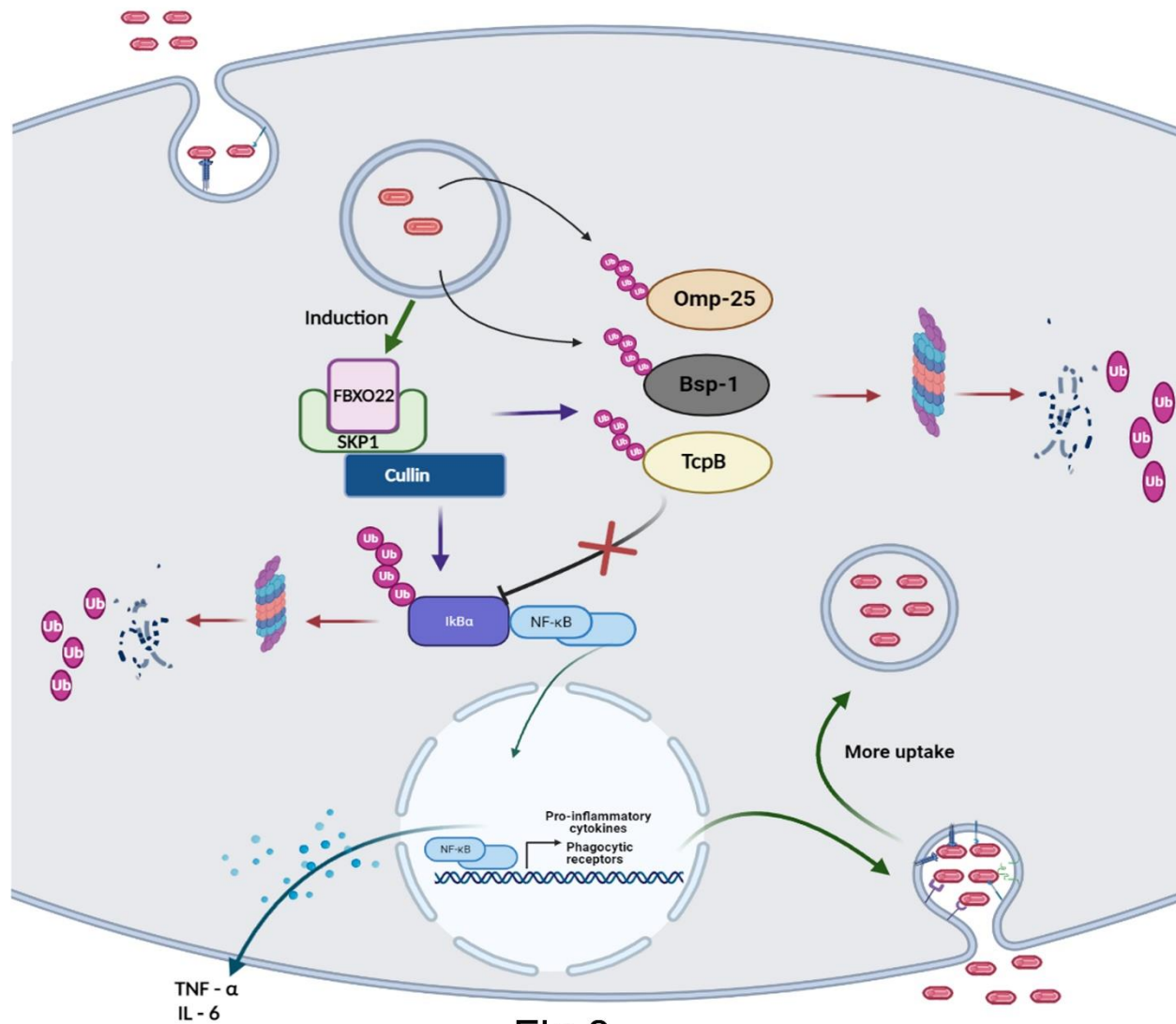
Fig 7

905

906

Fig 8

907

908

909

910

911

912

913

914

Figure captions

Figure 1. FBXO22 contributes to the macrophage infection of *Brucella* (A) CFU of *B. neotomae* in the control or FBXO22 silenced J774 macrophages after 24 hours of infection; (B) Number of intracellular *B. neotomae* in the control or FBXO22 silenced J774 macrophages at 4, 8, 12, 24 and 48 hours post-infection; (C) Confocal microscopic images of control or FBXO22 silenced J774 macrophages infected with *B.neotomae*-GFP. The images were captured 24 hours post-infection at 40X magnification. The cells were stained with anti-calreticulin primary antibody, followed by Alexa fluro 647-conjugated secondary antibody to visualize the endoplasmic reticulum (red). The nuclei were stained with DAPI (blue), which was present in the mounting reagent. Scale bar 20 µm. The right panel indicates quantification of intracellular *B neotomae*-GFP using FIJI software. The images are representatives of at least three independent experiments. (D) Overexpression of FBXO22 promotes macrophage infection of *B. neotomae.* J774 macrophages were transfected with empty vector or FBXO22 expression plasmid, followed by infection with *B. neotomae* and enumeration of CFU at 4, 8, 12 and 24 hours post-infection. The data are presented as mean $\pm$ SEM. from at least three independent experiments (*, $p < 0.05$; **, $p < 0.01$; ***, $p < 0.001$). NT: Non-targeting control; EV: Empty Vector; OE: Overexpression.

Figure 2. FBXO22 supports the invasion of *Brucella* into macrophages: (A) Invasion of *B. neotomae* into control or FBXO22-silenced J774 macrophages at 30, 60 and 90 minutes post-infection. The infected cells were treated with gentamycin (30 µg/ml) for 30 minutes after the indicated time points to kill extracellular bacteria, followed by CFU enumeration. **(B)** Confocal microscopic images of control or FBXO22 silenced J774 macrophages infected with *B.*

938   *neotomae*-GFP at 30 minutes post-infection. The red and blue fluorescence represent ER and

939   nuclei, respectively. Scale bar 20 µm. The right panel indicates quantification of intracellular *B.*

940   *neotomae*-GFP **(C)** *Brucella* invasion assay in J774 macrophages overexpressing FBXO22. J774

941   macrophages were transfected with EV or FBXO22 expression plasmid, followed by infection

942   with *B. neotomae* and enumeration of CFU at 30, 60 and 90 minutes post-infection as described

943   before. **(D)** β-TrCP does not affect the invasion of *Brucella* into macrophages. β-TrCP was over

944   expressed in J774 macrophages, followed by infection with *B. neotomae* and enumeration of

945   CFU at 30 minutes post-infection **(E & F)** Confirmation of FBXO22 knock-down by

946   CRISPR/dCas9 system by qRT-PCR (E) and by immunoblotting using anti-FBXO22 antibody

947   (F). Actin was used as the loading control. The intensity of FBXO22 band was measured using

948   Image J software and was normalized with Actin (right panel). **(G&H)** Infection of control or

949   FBXO22 knock-down J774 macrophages with *B. neotomae* (G) or *B. melitensis* (H), followed by

950   enumeration of CFU at 30, 60 and 90 minutes post-infection. **(I)** *Brucella* invasion assay using

951   J774 macrophages overexpressing GogB of *Salmonella*. J774 macrophages were transfected with

952   EV or GogB expression plasmid, followed by infection with *B. neotomae* and enumeration of

953   CFU at 30 minutes post-infection. The data are presented as $\pm$ SEM from at least three

954   independent experiments (*, $p < 0.05$; **, $p < 0.01$; ***, $p < 0.001$). The confocal and

955   immunoblot images are representatives of at least three independent experiments.

956   **Figure 3. Upregulation of FBXO22 in the *Brucella*-infected macrophages: (A)** Quantitative

957   qRT-PCR analysis of FBXO22 expression in the uninfected or *B. neotomae*-infected J774

958   macrophages. The cells were harvested at 0, 4, 8, 12 and 24 hours post-infection, followed by

959   RNA extraction, cDNA synthesis and qRT-PCR analysis. All data were normalized with

960   GAPDH and relative mRNA expression was quantified in comparison with uninfected for each

961   time point of infection **(B)** Immunoblot analysis of infected (upper panel) or *B. neotomae*

962   uninfected (lower panel) J774 cells. The cells were lysed at 0, 4, 8, 12, 24 and 48 hours post-

963   infection, followed by immunoblotting. The membrane was probed with anti-FBXO22 and anti-

964   Actin antibodies to detect endogenous levels of FBXO22 and Actin, respectively. The right panel

965   indicates the densitometry analysis of FBXO22 bands with respect to uninfected as control. The

966   band intensity was measured using Image J software and was normalized with Actin. The images

967   are representative of (n > 3) independent experiments; **(C)** Induction of FBXO22 in *B. neotomae*

968   infected macrophages at early time points. The expression of FBXO22 was analyzed by qRT-

969   PCR in the uninfected or *B. neotomae* infected J774 cells at 15, 30 and 60 minutes post-

970   infection. **(D)** Induction of FBXO22 in J774 macrophages infected with *B. melitensis.* qRT-PCR

971   analysis of FBXO22 expression in the uninfected or *B. melitensis* infected J774 macrophages at

972   indicated time points. **(E)** Induction of FBXO22 in J774 macrophages by LPS. The cells were

973   induced with 100 ng/ml LPS overnight, followed by immunoblotting analysis. The membrane

974   was probed using antibodies against FBXO22 and Actin. The right panel indicates the intensity

975   of FBXO22 band, which was normalized with Actin. **(F)** Expression level of FBXO22 in J774

976   macrophages induced with LPS for indicated time points. The expression was analysed using

977   qRT-PCR. All data were normalized with GAPDH and the relative mRNA expression was

978   quantified with respect to uninfected/uninduced control for each time point. Data are presented

979   as mean $\pm$ SEM. from at least three independent experiments (*, $p < 0.05$; **, $p < 0.01$; ***, $p <$

980   0.001).

981   **Figure 4. *Brucella* induces activation of NF-κB in the infected macrophages (A)** Luciferase

982   reporter assay to examine the activation of NF-κB. RAW264.7 were co-transfected with pNF-

983   κB–Luc reporter plasmid and the control plasmid, pRL-TK. Twenty-four hours post-transfection,

48

984 cells were infected with *B. neotomae* and the cells were collected at indicated time points,

985 followed by quantifying the luciferase activity. The data are represented as fold change of NF-κB

986 activation in the uninfected *vs* infected cells. **(B)** Degradation of IκBα in J774 macrophages

987 infected with *B. neotomae*. The levels of IκBα was analyzed by immunoblotting in *B. neotomae*

988 infected (upper panel) or uninfected (lower panel) at indicated time points. The right panel

989 indicate the densitometry of IκBα band, which was normalized with Actin. The images are

990 representative of three independent experiments **(C)** Inhibition of NF-κB by BAY 11-7082

991 suppresses invasion of *B. neotomae* into macrophages. J774 cells were pretreated with 10 μM of

992 DMSO or BAY 11-7082 for 2 hours, followed by infection with *B. neotomae* and CFU analysis

993 at 30, 60 and 90 minutes post-infection. **(D)** *Brucella* invasion assay in the presence of BAY 11-

994 7082 using *B. melitensis.* J774 or RAW 264.7 macrophages were pretreated with DMSO or BAY

995 11-7082 for 2 hours, followed by infection with *B. melitensis* and enumeration of CFU at 30

996 minutes post-infection. **(E)** Bay 11-7082 inhibits the enhanced invasion of *B. neotomae* into the

997 FBXO22 overexpressing macrophages. J774 macrophages that are transfected with EV or

998 FBXO22 expression plasmid was treated with DMSO or BAY 11-7082, followed by infection

999 with *B. neotomae* and enumeration of CFU at indicated time points. All the data are presented as

1000 mean $\pm$ SEM. from at least three independent experiments (*, p <0.05; **, p < 0.01; ***, p <

1001 0.001).

1002 **Figure 5. FBXO22 upregulates scavenger receptors on macrophages through NF-κB: (A &**

1003 **B)** The expression levels of indicated scavenger receptors in iBMDMs that are down-regulating

1004 (A) or overexpressing FBXO22 (B). iBMDMs were transfected with CRISPR-dCas9-gRNA

1005 plasmid for downregulating FBXO22 expression (A) or FBXO22 expression plasmid for

1006 overexpression of FBXO22 (B). The expression of levels of scavenger receptors was analyzed by

49

1007 qRT-PCR at 24 hours post-transfection. All data were normalized with GAPDH and the relative

1008 mRNA expression was quantified in comparison with EV CRISPR (EV CR) and EV for

1009 FBXO22 knock down and FBXO22 overexpression, respectively for each receptor. **(C)** BAY

1010 11-7082 suppresses induction of scavenger receptors. iBMDM were treated with 10 µM of BAY

1011 11-7082 for 2 hours, followed by qRT-PCR analysis using receptor specific primers. All data

1012 were normalized with GAPDH and relative mRNA expression was quantified in comparison

1013 with DMSO treated cells for each receptor. **(D)** Scavenger receptors are upregulated in *B.*

1014 *neotomae* infected macrophages. The expression levels of scavenger receptors are examined in

1015 the uninfected or *B. neotomae* infected iBMDMs for the indicated time points. All data were

1016 normalized with GAPDH and relative mRNA expression of each receptor was quantified in

1017 comparison with uninfected for indicated time points. **(E)** Enhanced invasion *B. neotomae* upon

1018 re-infection of infected macrophages. BMDMs were infected with *B. neotomae* for 2 or 4 hours,

1019 followed by analyzing the invasion of *B. neotomae* into the infected macrophages. The CFU of

1020 *B. neotomae* was enumerated at 30 minutes post-invasion after killing the extracellular bacteria

1021 by gentamycin treatment; **(F)** Fluorescent microscopic image of iBMDMs infected with *B.*

1022 *neotomae* for 2 or 4 hours, followed by analyzing the invasion of *B. neotomae*-tdTomato (red)

1023 into the infected macrophages. The infected cells were analyzed for invasion of *B. neotomae*-

1024 tdTomato 30 minutes post-infection. The cell nuclei were stained using Hoechst (Blue). The

1025 spot count of number of *B. neotomae*-tdTomato (red) was measured using FIJI software (right

1026 panel). Scale bar 20 µm. The fluorescence images are representatives of at least three

1027 independent experiments. The relative expression was normalized with mouse GAPDH in qRT-

1028 PCR assays. All the data are presented as mean $\pm$ SEM. from at least three independent

1029 experiments (*, $p < 0.05$; **, $p < 0.01$; ***, $p < 0.001$).

1030   **Figure 6.** *Brucella*-**induced upregulation of FBXO22 results enhanced secretion of TNF-α**

1031   **by macrophages**. **(A-D)** Quantification of *B. neotomae*-induced production of TNF-α (A & C)

1032   and IL-6 (B & D) in J774 macrophages at indicated time intervals by qRT-PCR (A & B) and

1033   ELISA (C & D). The qRT-PCR data were normalized with GAPDH and relative mRNA

1034   expression was quantified with respect to uninfected for each time point of infection; **(E-F)**

1035   Quantification of *B. melitensis*-induced of production of TNF-α (E) and IL-6 (F) in J774 cells at

1036   indicated time intervals by ELISA; **(G-H)** Overexpression of FBXO22 enhances the production

1037   of TNF α and IL-6 in *Brucella*-infected macrophages. J774 cells were transfected with FLAG-

1038   FBXO22 expression plasmid or empty vector, followed by infection with *B. neotomae* for

1039   indicated time points and quantification of secreted TNF-α **(G)** and IL-6 **(H)** using ELISA; **(I-J)**

1040   BAY-117082 suppresses enhanced production of TNF-α and IL-6 in FBXO22 overexpressed

1041   cells. J774 cells were transfected with MYC-FBXO22, followed by treatment with BAY-117082

1042   and infected with *B. neotomae for* indicated time points. The expression levels of TNF-α (I) and

1043   IL-6 (J) were quantified using qRT-PCR. All data were normalized with GAPDH and relative

1044   mRNA expression was quantified with respect to EV+DMSO for indicated time points **(K-L)**

1045   BAY 11-7082 suppresses TNF-α and IL-6 production in macrophages. J774 cells were pretreated

1046   with 10 μM of DMSO or BAY 11-7082 for 2 hours, followed by infection with 100 or 1000

1047   MOI of *B. neotomae* and quantification of mRNA expression levels of TNF-α **(K)** and IL-6 **(L)**

1048   using qRT-PCR. All data were normalized with GAPDH and relative mRNA expression was

1049   quantified with respect to DMSO treated cells for each MOI. The data are presented as mean $\pm$

1050   SEM. from at least three independent experiments (*, $p < 0.05$; **, $p < 0.01$; ***, $p < 0.001$).

1051

1052 **Figure 7. (A)** FBXO22 interacts with TcpB. Lysate of HEK293 cells overexpressing FLAG-

1053 FBXO22 was mixed with purified MBP-TcpB or MBP alone, followed by immunoprecipitation

1054 of FLAG-FBXO22 using anti-FLAG antibody and immunoblotting. Anti-MBP antibody was

1055 used to detect co-immunoprecipitated MBP-TcpB; **(B)** FBXO22 promotes degradation of TcpB.

1056 HEK293T cells were co-transfected with HA-TcpB and increasing concentrations of MYC-

1057 FBXO22 plasmids. Twenty-four hours post transfection, cells were lysed and subjected to

1058 immunoblotting. The blot was probed with anti-HA and anti-MYC antibodies to detect HA-

1059 TcpB and MYC-FBXO22, respectively. Actin served as the loading control. Right panel

1060 indicates the densitometry of HA-TcpB band, which was normalized with Actin. **(C & D)**

1061 Silencing of FBXO22 prevents the degradation of TcpB. FBXO22 was silenced in HEK293T

1062 cells using siFBXO22 (C), followed by transfection with HA-TcpB and immunoblotting (D).

1063 The blot was probed with anti-HA and anti-FBXO22 to detect HA-TcpB and FBXO22,

1064 respectively. Right panels indicate the densitometry of HA-TcpB or FBXO22 band, which was

1065 normalized with Actin; **(E)** *S. typhimurium* infection prevents degradation of TcpB. HEK293T

1066 cells were co-transfected with FBXO22 and TcpB, followed by infecting the cells with

1067 *Salmonella typhimurium*. Twenty-four hours post transfection/infection, cells were lysed and

1068 subjected to immunoblotting. The blot was probed with anti-HA and anti-MYC antibodies to

1069 detect HA-TcpB and MYC-FBXO22, respectively. Actin served as the loading control. The right

1070 panel indicates band intensity of HA-TcpB that was normalized with Actin. **(F&G)** Silencing of

1071 SKP1 affects the degradation of TcpB. SKP1 was silenced in HEK293T cells (F), followed by

1072 transfection with HA-TcpB and immunoblotting (G). The right panel indicates the band

1073 intensity of HA-TcpB that was normalized with actin. **(H)** β-TrCP does not induce degradation

1074 of TcpB. HEK293T cells were co-transfected with HA-TcpB and increasing concentrations of

1075   MYC-β-TrCP plasmids. Twenty-four hours post transfection, cells were lysed and subjected to

1076   immunoblotting. The blot was probed with anti-HA and anti-MYC antibodies to detect HA-

1077   TcpB and MYC-β-TrcP, respectively. Actin served as the loading control. The right panel

1078   indicates band intensity of HA-TcpB that was normalized with Actin. **(I)** FBXO22 induces

1079   enhanced ubiquitination of TcpB. HEK293T cells were co-transfected with FLAG-TcpB, MYC-

1080   FBXO22, and HA-ubiquitin as indicated. Twenty-four hours post transfection, cells were lysed

1081   and FLAG-TcpB was immunoprecipitated, followed by immunoblotting. Probing of the blot

1082   with anti-HA antibody detected HA-ubiquitin–conjugated FLAG-TcpB. **(J-K)** FBXO22

1083   promotes degradation of other effector proteins of *Brucella*. HEK293T cells were co-transfected

1084   with increasing concentrations of FBXO22 and equal concentration of HA-OMP25 (J) or FLAG-

1085   Bsp1 (K). Twenty-four hours post transfection, cells were lysed and subjected to

1086   immunoblotting. The blots were probed with ant-HA, anti-FLAG and anti-MYC antibodies to

1087   detect OMP25, BSP1 and FBXO22, respectively. The right panel indicates the band intensity of

1088   HA-tagged proteins that were normalized with Actin.

1089   **Figure 8. Role of FBXO22 in the enhanced uptake of *Brucella* and induction of**

1090   **inflammatory cytokines.** Invasion of *Brucella* induces the expression of FBXO22 in

1091   macrophages that in turn promotes NF-κB activation and enhanced expression of scavenger

1092   receptors and production of pro-inflammatory cytokines. FBXO22 also induces the degradation

1093   of effector proteins of *Brucella* through the SCF-complex.

1094